

INFRARED SPECTROSCOPIC STUDIES OF MATRIX-ISOLATED GUANINES:
EVIDENCE OF TAUTOMERIC EQUILIBRIA

BY

LUIS A. HERNANDEZ-VILLARINI

A DISSERTATION PRESENTED TO THE GRADUATE SCHOOL
OF THE UNIVERSITY OF FLORIDA IN
PARTIAL FULFILLMENT OF THE REQUIREMENTS
FOR THE DEGREE OF DOCTOR OF PHILOSOPHY
UNIVERSITY OF FLORIDA

1987

To

My wife Mayra and my mother Concepcion.

ACKNOWLEDGEMENTS

I would like to express my deepest gratitude to Dr. Willis B. Person, without whom this work would not have been possible. His patience, understanding and guidance have been the primary inspiration for this work.

I am grateful to Dr. Krystina Szczepaniak, formerly of the Polish Academy of Sciences (Warsaw, Poland) for her friendship and helpful discussions. Thanks are due to Dr. Marian Szczesniak and Dr. Martin Vala for sharing their knowledge and expertise with the matrix-isolation equipment and techniques.

I am also grateful to all the past and present members of this research group for their friendship over the years. Special thanks are due to Mr. Dennis Roser for his help with the FT-IR.

The partial support from the National Institute of Health (Grant No. GM-32988) is gratefully acknowledged.

TABLE OF CONTENTS

	<u>Page</u>
ACKNOWLEDGEMENTS	iii
LIST OF TABLES	vi
LIST OF FIGURES	vii
ABSTRACT	x
 CHAPTERS	
I INTRODUCTION	1
Statement of the Problem	1
Purines and Pyrimidines: Natural Occurrence and Biological Importance.....	2
The Principal Types of Tautomerism in Heteroatomic Compounds	9
The Importance of Tautomerism in Nucleic Acid Bases	13
Effect of Environment on Tautomeric Equilibria	15
II LITERATURE REVIEW	18
Tautomerism of Pyrimidine Bases	18
Tautomerism of Purine Bases	23
III EXPERIMENTAL SECTION	32
Matrix-Isolation: Advantages and Disadvantages	32

Preparation of Low-Temperature Matrices	37
Materials and Equipment	46
IV RESULTS AND DISCUSSION	48
Infrared Spectra of Matrix-Isolated Guanine and Derivatives	48
The 3600-3400 cm^{-1} Region	73
The 1800-700 cm^{-1} Region	81
V CONCLUSION AND RECOMMENDATIONS	94
APPENDICES	
A. Infrared Survey Spectra in the 3900-700 cm^{-1} Region	100
B. Infrared Spectra of Isolated Molecules in Argon and Nitrogen Matrices in the 3600-3400 cm^{-1} Region	122
C. Infrared Spectra of Isolated Molecules in Argon and Nitrogen Matrices in the 1800-700 cm^{-1} Region	128
REFERENCES	154
BIOGRAPHICAL SKETCH	164

LIST OF TABLES

<u>TABLE</u>	<u>Page</u>
I Principal Types of Tautomerism in Heteroatomic Compounds	10
II Experimental Parameters and Source of the Compounds Under Study	41
III Frequencies and Assignments of the Bands in the Infrared Spectra of 1,7-dimethylguanine in Argon and Nitrogen Matrices, Amorphous Solid at 10 K and KBr Pellets	54
IV Frequencies and Assignments of the Bands in the Infrared Spectra of 7-methylguanine in Argon and Nitrogen Matrices, Amorphous Solid at 10 K and KBr Pellets	57
V Frequencies and Assignments of the Bands in the Infrared Spectra of 2-N,N-dimethylaminoguanine in Argon and Nitrogen Matrices, Amorphous Solid at 10 K and KBr Pellets	60
VI Frequencies and Assignments of the Bands in the Infrared Spectra of 9-ethylguanine in Argon and Nitrogen Matrices, Amorphous Solid at 10 K and KBr Pellets	64
VII Frequencies and Assignments of the Bands in the Infrared Spectra of Guanine in Argon and Nitrogen Matrices, Amorphous Solid at 10 K and KBr Pellets .	68
VIII Tautomeric Forms of Guanine and Its Derivatives in Argon and Nitrogen Matrices and in the Solid State	97

LIST OF FIGURES

<u>FIGURE</u>	<u>Page</u>
1. A Random Segment of a Nucleic Acid and Its Constituent Parts	4
2. Structure of Common Purines and Pyrimidines	5
3. Double-Helical Structures of DNA, RNA, and DNA/RNA Hybrids	7
4. Watson-Crick Base-Pairing Scheme	8
5. Classification of Possible Types of Tautomerism in Neutral Heteroatomic Molecules	12
6. Tautomeric Forms of Uracil	19
7. Tautomeric Forms of Cytosine	21
8. Tautomeric Forms of Purine	24
9. Amino-Imino Tautomerism in Adenine	25
10. Oxo-Hydroxy Tautomerism in Hypoxanthine	26
11. Vacuum Shroud Arrangement	37
12. Schematics of Experimental Set-Up	39
13. Infrared Spectra of 9-ethylguanine in the Solid State	43
14. Tautomeric Forms of 1,7-dimethylguanine	49
15. Tautomeric Forms of 7-methylguanine	50
16. Tautomeric Forms of 2-N,N-dimethylaminoguanine .	51
17. Tautomeric Forms of 9-ethylguanine	52

18.	Tautomeric Forms of Guanine	53
19.	Infrared Spectra of Guanine and Its Derivatives in the 3600-3400 Wavenumber Region	74
20.	Infrared Spectra of Guanine and Its Derivatives in the 1800-700 Wavenumber Region	83
21.	"Correct" G-C Pair and "Incorrect" G*-U Pair	95
A.1	Infrared Survey Spectrum of 1,7-dimethylguanine Isolated in an Argon Matrix	101
A.2	Infrared Survey Spectrum of 1,7-dimethylguanine Isolated in a Nitrogen Matrix	102
A.3	Infrared Survey Spectrum of a Polycrystalline Film of 1,7-dimethylguanine Deposited at 10 K ...	103
A.4	Infrared Survey Spectrum of 1,7-dimethylguanine in the Solid State (KBr Pellet)	104
A.5	Infrared Survey Spectrum of 7-methylguanine Isolated in an Argon Matrix	105
A.6	Infrared Survey Spectrum of 7-methylguanine Isolated in a Nitrogen Matrix	107
A.7	Infrared Survey Spectrum of a Polycrystalline Film of 7-methylguanine Deposited at 10 K	108
A.8	Infrared Survey Spectrum of 7-methylguanine in the Solid State (KBr Pellets)	109
A.9	Infrared Survey Spectrum of 2-N,N-dimethylamino- guanine Isolated in an Argon Matrix	110
A.10	Infrared Survey Spectrum of 2-N,N-dimethylamino- guanine Isolated in a Nitrogen Matrix	111
A.11	Infrared Survey Spectrum of a Polycrystalline Film of 2-N,N-dimethylaminoguanine Deposited at 10 K	112
A.12	Infrared Survey Spectrum of 2-N,N-dimethylamino- guanine in the Solid State (KBr Pellets)	113
A.13	Infrared Survey Spectrum of 9-ethylguanine Isolated in an Argon Matrix	114

A.14	Infrared Survey Spectrum of 9-ethylguanine Isolated in a Nitrogen Matrix	115
A.15	Infrared Survey Spectrum of a Polycrystalline Film of 9-ethylguanine Deposited at 10 K	116
A.16	Infrared Survey Spectrum of 9-ethylguanine in the Solid State (KBr Pellets)	117
A.17	Infrared Survey Spectrum of Guanine Isolated in an Argon Matrix	118
A.18	Infrared Survey Spectrum of Guanine Isolated in a Nitrogen Matrix	119
A.19	Infrared Survey Spectrum of a Polycrystalline Film of Guanine Deposited at 10 K	120
A.20	Infrared Survey Spectrum of Guanine in the Solid State (KBr Pellets)	121
B.1	Infrared Spectra of 1,7-dimethylguanine Isolated in Argon and Nitrogen Matrices	123
B.2	Infrared Spectra of 7-methylguanine Isolated in Argon and Nitrogen Matrices	124
B.3	Infrared Spectra of 2-N,N-dimethylaminoguanine Isolated in Argon and Nitrogen Matrices	125
B.4	Infrared Spectra of 9-ethylguanine Isolated in Argon and Nitrogen Matrices	126
B.5	Infrared Spectra of Guanine Isolated in Argon and Nitrogen Matrices	127
C.1	Infrared Spectra of 1,7-dimethylguanine Isolated in Argon and Nitrogen Matrices	129
C.2	Infrared Spectra of 7-methylguanine Isolated in Argon and Nitrogen Matrices	134
C.3	Infrared Spectra of 2-N,N-dimethylaminoguanine Isolated in Argon and Nitrogen Matrices	139
C.4	Infrared Spectra of 9-ethylguanine Isolated in Argon and Nitrogen Matrices	144
C.5	Infrared Spectra of Guanine Isolated in Argon and Nitrogen Matrices	149

Abstract of Dissertation Presented to the Graduate School
of the University of Florida in Partial Fulfillment of the
Requirements for the Degree of Doctor of Philosophy

INFRARED SPECTROSCOPIC STUDIES OF MATRIX-ISOLATED GUANINES:
EVIDENCE OF TAUTOMERIC EQUILIBRIA

BY

LUIS A. HERNANDEZ-VILLARINI

DECEMBER 1987

Chairman: Willis B. Person
Major Department: Chemistry

Infrared absorption spectra have been obtained for matrix-isolated guanine and 9-ethylguanine (a formal analogue of the natural nucleoside found in DNA and RNA) in argon and nitrogen matrices. Three other derivatives, 7-methylguanine, the fixed oxo-derivative 1,7-dimethylguanine, and the fixed amino-derivative 2-N,N-dimethylaminoguanine have also been examined. The spectra provided evidence of the existence of guanine, 9-ethylguanine, and 2-N,N-dimethylaminoguanine as mixtures of their amino-oxo and amino-hydroxy tautomers, although the amino-oxo tautomer is the only tautomeric form found in solution and in the solid state. The effect of substituents (methylation at the N(7)- or the N(9)-position) was clearly established through the comparison of the infrared spectra of 7-methylguanine to that of 9-ethylguanine. While both the amino-oxo and the amino-hydroxy

forms were detected for 9-ethylguanine only the amino-oxo form was detected for 7-methylguanine. The stabilization of the hydroxy form by intramolecular hydrogen-bonding between the O-H and the lone pair of the nitrogen at the N(7)-position was postulated.

The significance of these results are evaluated in relation to the types of tautomers found in natural nucleic acids and to the concept of spontaneous and induced mutations caused by mispairing of the nucleic acid bases.

CHAPTER I

INTRODUCTION

Statement of the Problem

The purpose of this study is to present experimental data on the tautomerism of guanine, particularly of nucleic acid analogue 9-ethylguanine and some other derivatives. Considerable attempts have been made in an effort to understand the phenomenon of tautomerism, not only in relation to quantitative concepts of chemical binding and structure-activity relationships in organic and physical chemistry (1-4), but also in relation to spontaneous mutations as a consequence of mispairing by rare tautomeric forms of purines and pyrimidines (4-7), or in relation to enzyme-substrate interactions (8). Such tautomerism is also of major significance in the structure of nucleic acids and is of current additional importance in relation to anti-metabolic (including antitumor and antiviral) activities of nucleoside and nucleotide analogues (9-13). Recent developments, including the ability to evaluate tautomeric equilibria for nitrogen heterocycles in the gas phase (14-16), as well as in low-temperature matrices (14,15,17-29),

provide for the first time data for valid comparisons with theoretical calculations. They also furnished a solid foundation for quantitatively evaluating the effect of the environment on tautomeric equilibria (30).

Purines and Pyrimidines: Natural Occurrence and Biological Importance

Purines and pyrimidines are major chemical constituents of living cells and occur primarily as components of polymerized nucleotides (nucleic acids), and to a much lesser extent in the form of "free" (that is unassociated) nucleotides (10,11,31). Free nucleosides and bases usually represent a very small fraction of the total purine and pyrimidine content of living cells (9-11). However, there are exceptions to this generalization, such as the occurrence of substantial amounts of theophylline, theobromine, and caffeine in some plant tissues (9,10), and the occurrence of the arabinoside of thymine and uracil in the Caribbean sponge, *Cryptotethia crypta* (10).

Other purine and simple purine derivatives that abound in nature are mainly of the oxo and amino type. Perhaps the most widespread are related to adenine. Adenine occurs in the free form, for example, in human urine along with xanthine (and its methylated forms) and hypoxanthine, in human feces together with hypoxanthine, xanthine, and guanine, and with guanine in cow's milk (9,10). It is also found as the free base in many plants (10).

When nucleic acids are subjected to complete chemical hydrolysis, there are obtained, ideally, mixtures containing one mole of phosphate, one mole of sugar, and one mole of a mixture of heterocyclic bases (11). If the chemical hydrolysis is performed under milder conditions or by enzymatic means, and equimolar mixture of nucleosides or the corresponding set of nucleotides is obtained (11). Nucleotides are the true monomeric units of the nucleic acids (See Figure 1).

The bases found in nucleic acids are either pyrimidines or purines. In DNA the common bases are the pyrimidines thymine (T) and cytosine (C) and the purines adenine (A) and guanine (G). Some methylcytosine occurs occasionally, especially in the DNA of higher plants (e.g., wheat germ) and certain bacteria; 6-methylaminopurine is a minor constituent of DNA of bacterial viruses (bacteriophages); and uracil and 5-hydroxymethyluracil have been reported as occurring in certain bacteriophage DNA (9,11). A particular class of bacteriophages, the so-called T-even phages of "Escherichia coli", contains 5-hydroxymethylcytosine in place of cytosine (9,11). The structure of these bases is shown in Figure 2.

Most RNAs also contain only four bases: the purines adenine (A) and guanine (G) and the pyrimidines uracil (U) and cytosine (C) (9,11). In some RNAs, hypoxanthine and various methylated bases, such as thymine, 5-methylcytosine, 6-methylaminopurine (and its 6,6-dimethyl-derivative), as well

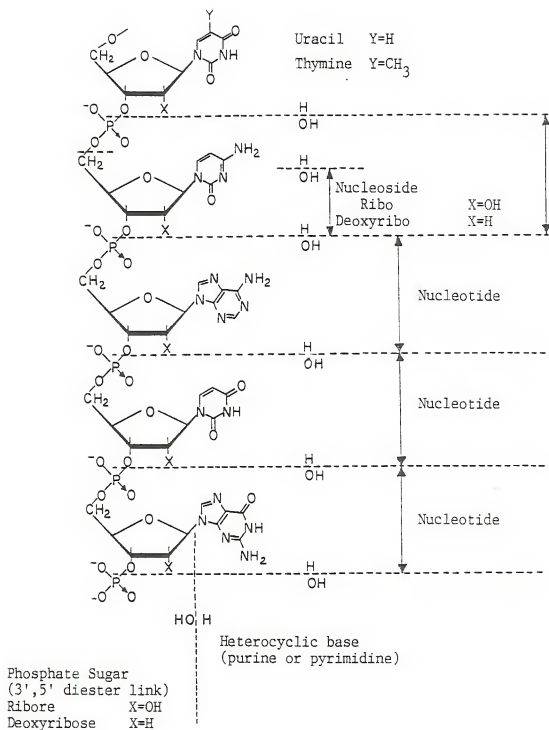


Figure 1. A Random Segment of a Nucleic Acid and Its Constituent Parts.

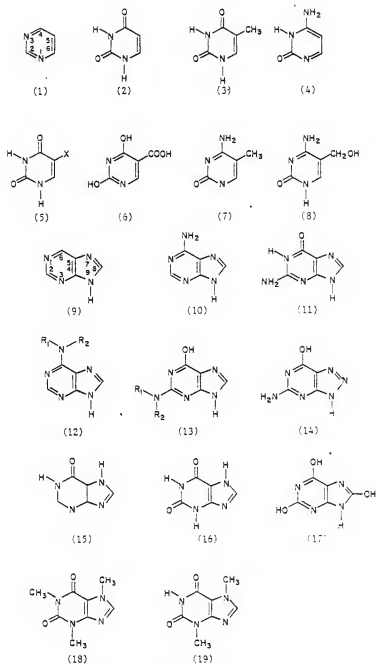


Figure 2. Structure of Common Pyrimidines and Purines: (1) Pyrimidine, (2) Uracil, (3) Thymine, (4) Cytosine, (5) Halogenated Uracil (X=F, Br, I), (6) Orotic Acid, (7) 5-methylcytosine, (8) 5-hydroxymethylcytosine, (9) Purine, (10) Adenine, (11) Guanine, (12) 6-methylamino- and 6,6-dimethylaminopurine, (13) 2-methyl- and 2,2-dimethylamino-6-hydroxypurine, (14) 8-azaguanine, (15) Hypoxanthine, (16) Xanthine, (17) Uric Acid, (18) Caffeine, (19) Theobromine.

as dihydrouracil and some others, replace some of the normal constituents (11). The methylated bases in RNA and DNA appear to be formed as a result of methylation of intact polymeric nucleic acids rather than of component monomeric units (11).

The unique structures and properties of nucleic acids are due largely to specific interactions among purine and pyrimidine bases. These interactions appear to be primarily of two types: hydrogen-bonding and base stacking. With exceptions, deoxyribonucleic acid (DNA), usually forms a perfect double-helix composed of two individual right-handed helices (11,13). The structure is that of the bases in one chain paired with the complementary bases in the other chain (see Figure 3). Guanine-cytosine and adenine-thymine (or uracil in RNA) are the standard complementary or Watson-Crick pairs (32,33).

The base pairs are determined by hydrogen bonds between certain atoms in each base (see Figure 4). These bonds are strongly responsible for the replication and transfer of information from the helix. However, an energetically more important role is played by the water repulsion of internally stacked bases, which are hydrophobic compared to the exposed hydrophilic phosphate backbone. The nonpolar stacking of bases creates mutually attracting van der Waals (or London) and electrostatic forces which stabilize the helix (34).

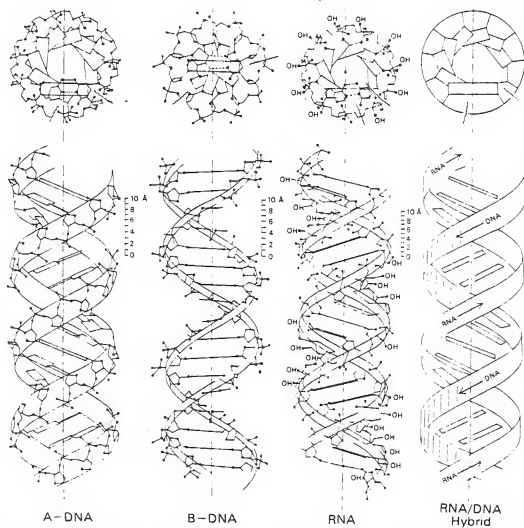


Figure 3. Double-Helical Structures for DNA, RNA, and DNA/RNA Hybrids.
From Reference 35.

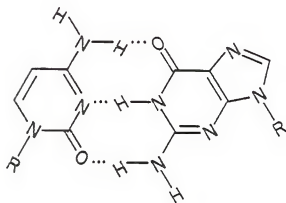
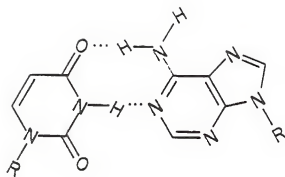


Figure 4. Watson-Crick Base Pairing Scheme.

DNA in aqueous solution is therefore a rigid and thermodynamically stable molecule that never breaks apart, except reversibly for a few terminal nucleotides (11,34,35). The higher the proportion of guanine-cytosine pairs, the more stable the molecule.

It is now well established that the genetic code of living organism is contained in the nucleic acids (DNA and RNA) as a linear sequence of four different bases: adenine (A), guanine (G), cytosine (C), and thymine (T) in DNA or uracil (U) in RNA (11). Although these bases can potentially exist in various tautomeric forms, in fact it is generally accepted that they do exist in one stable structure characteristic for each base and constitute specific purine-pyrimidine pairs in the DNA helix. However, the possible appearance of DNA bases in their unusual tautomeric forms can increase the probability of mispairing of the pyrimidines and purines and hence may lead to mutations (4-7).

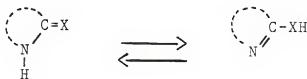
The Principal Types of Tautomerism in Heteroatomic Compounds

The prototropic tautomerism of heteroatomic compounds comprises all the cases where a mobile atom can move from one site to another in a heteroatomic molecule (3). The most common type involves the movement of a proton between a cyclic atom and a substituent atom directly connected to the ring. A classification of the possible types of tautomerism is shown in Figure 5 and Table I. The top row in Figure 5 shows the various sites available; (A) a cyclic sp^2 -

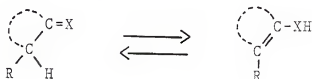
TABLE I

Principal Types of Tautomerism in Heteroatomic Compounds

- A. Annular nitrogen and an atom adjacent to the ring.
- ^a



- B. Annular carbon and an atom adjacent to the ring.



- C. Two atoms adjacent to the ring.



- D. Two annular nitrogen atoms.

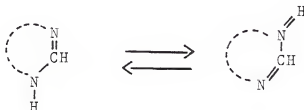
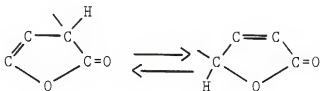


TABLE I-continued.

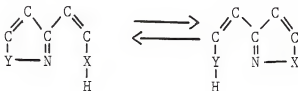
E. Two annular carbon atoms.



F. Annular carbon and nitrogen atoms.



G. Rearrangements.



H. Ring-chain tautomerism.

^aFrom reference 3.

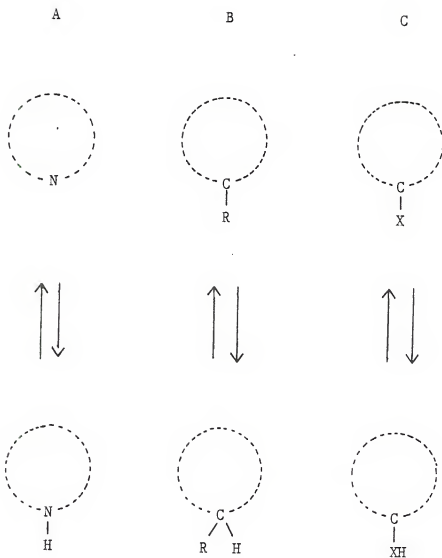


Figure 5. Classification of possible types of tautomerism in neutral heteroatomic molecules.

hybridized nitrogen; (B) an sp^2 -hybridized ring carbon; and (C) and sp^2 -hybridized atom directly attached to a ring nitrogen. The lower row of figures in Figure 5 shows the corresponding potential sites from which a proton can be removed. Any heteroatomic molecule which contains at least one site of the type shown in the lower row together with one of the types shown in the upper row is capable of tautomerism (3).

The Importance of Tautomerism in Nucleic Acid Bases

A number of chemical alterations of DNA may lead to its loss or change of function (36). The list includes such obvious changes as backbone breakage or cross-linking of the two chains, which prevents them from separating for replication purposes. Less severe chemical changes, such as base alterations, may also block the action of the enzymes that copy DNA sequences into a new DNA or RNA bonding pattern so that it pairs with a substance other than its normal Watson-Crick partner (11,36). Other types of changes may lead to frameshift mutations, with more drastic alterations in protein sequence, or to large deletions, with loss of genetic information (11,36).

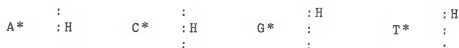
Genetic information may be defined as that primarily required to assemble a protein, hence ultimately required to perpetuate biological orders. It is well known that the accuracy of the transfer of genetic information during DNA replication and RNA transcription for protein synthesis

relies on the unique base pairing of the complementary nucleic acid bases (33,34). The specificity of the bonding concerns both this exclusiveness and the steric arrangement which is depicted in Figure 4. It is easy to see that the existence of the complementary pairing necessitates the simultaneous presence of the bases in definite tautomeric forms, namely oxo and amino forms, and it is only with such complementary forms that the appropriate hydrogen bonds may be formed.

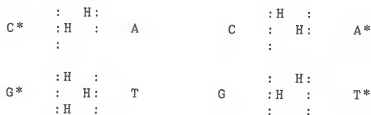
Considering only the possible H-bonds in the specific positions of the bases, one obtains the following proton-electron pair code for the four bases involved, which immediately indicates A-T, and G-C as the only possible combination:



Associated with these scheme is, however, the observation that if a base happens to exists in one of its rare tautomeric forms; imino for adenine and cytosine and/or hydroxy for guanine and thymine (denoted by A*, C*, G*, and T*, respectively) this could lead to mispairing of the bases (4-7). Thus the short-hand proton-electron pair codes would then be modified as follows:



Therefore cytosine in its imino form would be able to H-bond to adenine in its amino form (and vice versa) and guanine in its hydroxy form would couple with thymine in its oxo form (and vice versa):



As a result of such miscoupling, the original order of the arrangement of successive base pairs along the axis of the nucleic acid would be modified and the modification perpetuated during DNA replication. The order of the complementary base pairs along the axis of DNA being most probably responsible for the genetic code, any perturbation to this order represents by definition a mutation (36).

Effect of Environment on Tautomeric Equilibria

The influence of molecular environment on tautomerism in purines and pyrimidines is directly relevant to the role of these heterocyclic compounds in nucleic acid structure and function. The nucleic acid bases exist, under physiological conditions, in aqueous media. However, following incorporation into nucleic acids, they are frequently in the

aprotic environment prevailing in the interior of the double-helical structure. The striking role of the molecular environment on tautomeric equilibria has been well documented (1,3,37-49). In particular it has been shown that the vapor phase protomeric equilibrium constants for oxo- and mercapto-pyridines (41-44,47,49), and pyrimidines (41,45,49), may differ from the corresponding equilibrium constants for such systems in solution by factors of the order of $10^3 - 10^5$.

Apart from gas phase studies, solvent and association effects may also be minimized in low-temperature matrices consisting of argon and other relatively inert gases (12,30). These matrix-isolation studies are of relevance in the analysis of the effects of weakly interacting aprotic environment on the tautomeric equilibria, thus bridging the gap between data for the gas phase and for polar solvents. It should be noted that information about such equilibria in polar solvents is somewhat limited due primarily to solubility considerations.

Another additional advantage of the infrared matrix-isolation technique is that absorption bands of the isolated species are fairly sharp, thus allowing resolution of bands with small frequency differences which usually overlap in solution and in the vapor phase (see section on Matrix-Isolation discussed later). Infrared spectroscopy, which permits direct observation of C=O, O-H, and N-H absorption bands involved in oxo-hydroxy tautomerism, have been shown to

provide results more reliable than those obtained by ultraviolet spectroscopy (14,44,45).

Infrared absorption spectra have been reported for 4-oxo-6-methyl- and 2-oxo-4,6-dimethylpyrimidines and several related derivatives in the gas phase, in low-temperature matrices, and in several liquid solvents (14). All the oxo-pyrimidines in the gas phase, and 4-oxo-6-methylpyrimidine in low-temperature matrices were found to exhibit comparable populations of the oxo and hydroxy forms. By contrast the hydroxy tautomers prevailed as the predominant form in both the gas phase and low-temperature matrices in the 2-oxo-pyrimidines (14). Both classes of compounds were found to exist predominantly in their oxo form in liquid solvent systems such as toluene, hexane, carbon tetrachloride and deuteriochloroform (14). Equilibrium constant ($K_T = [NH/OH]$) values of 2 for 4-oxo-2,6-dimethylpyrimidine and 1 for the other 4-oxopyrimidines in the vapor phase were reported (14). The same equilibrium constants in inert matrices were found to vary slightly with the activity of the matrix gas (Ar, Kr, CO₂, C₆H₁₄, CCl₄, CDCl₃, C₆H₅CH₃), with the oxo tautomer favored in the more active matrix (14). These results are consistent with previous studies of the effect of the medium on protomeric equilibria in solution: as the polarity of the medium increases, the more polar tautomer is stabilized relative to the less polar tautomer (47).

CHAPTER II

LITERATURE REVIEW

Tautomerism of Pyrimidine Bases

Uracil (or thymine, its 5-methyl derivative) can exist in six tautomeric forms (see Figure 6). A large amount of experimental evidence shows that uracil and thymine have the dioxo (dilactam) structure (tautomeric form 1 in Figure 6). This form was found in X-ray crystallographic studies of uracil (50,51), and thymine (52,53), and of derivatives of these molecules (54-63). Analysis of the infrared spectra of uracil, thymine, their nucleotides and nucleosides, confirms the predominance of tautomeric form 1 (see Figure 6) in the solid state as well as in solution (64-74). Raman spectroscopic studies confirmed the conclusion from infrared spectroscopy by showing that uracil and uridine possess the dioxo form (73,75,76). Several NMR and NQR studies performed in search of the predominant tautomeric structures of uracil and thymine, their nucleotides and nucleosides, indicated that the dioxo structure predominates in uracil compounds in

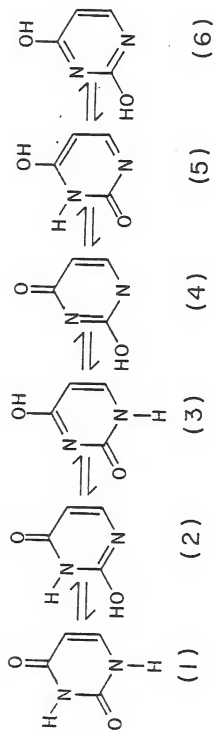


Figure 6. Tautomeric Forms of Uracil

aqueous and non-aqueous solutions as well as in the solid state (77-82).

The infrared absorption spectra of 1-substituted uracils in the vapor phase showed no absorption bands in the hydroxyl region ($3700\text{--}3500\text{ cm}^{-1}$) pointing to the existence of these derivatives in the dioxo form (16). Infrared matrix-isolation studies on uracil monomers (17,19,22,23), deuterated- (23), and methylated- derivatives of uracils (20,21), also could not identify absorption bands arising from hydroxyl group vibrations, thus providing further evidence pointing to the 2,4-dioxo tautomer as the sole species in uracil vapors.

Compelling evidence exists for the predominance of the amino-oxo structure of cytosine (tautomeric form 1 in Figure 7) in the solid state. X-ray crystal analysis on cytosine (82-85), its complexes with different partners (86-91), and citidine-2',3'-cyclicphosphate (93), all indicated its existence in the amino-oxo form. Early infrared spectroscopic studies were inconclusive; some were considered to indicate that cytosine exists in the amino-hydroxy form 3 (see Figure 7) in the solid state (94,95), others that it exists in the amino-oxo form 1 or 2 (64,65,96). More recent studies on cytidine, 5-halo-deoxycytidine, sodium cytidilate, and polycytidylic acid in neutral H_2O or D_2O solutions advocate tautomeric form 1 for the cytosine residue (66-69, 97-102).

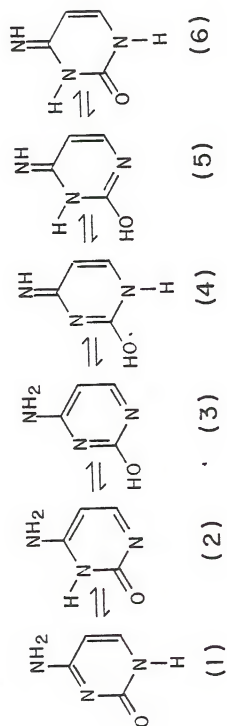


Figure 7. Tautomeric Forms of Cytosine.

The conclusions from infrared spectroscopy have been confirmed by Raman spectroscopic studies on the constituent bases of RNA, their nucleosides and nucleotides, and some related model compounds (75,76,97). The Raman spectra of cytosines rule out the prevalence of the imino form 6 (see Figure 7) in aqueous solution and indicate that the neutral molecules have the amino-oxo form 1.

Indirect arguments such as comparison of pK values of various methylated derivatives of cytosine, have shown that in aqueous solution the amino-oxo form with the hydrogen at the N(1)-position (tautomeric form 1 in Figure 7) is expected to predominate over the amino-oxo form with the hydrogen at the N(3)-position (tautomeric form 2 in Figure 7), and the imino-oxo form by factors of 800 and $10^4 - 10^5$, respectively (103). Similar conclusions have been drawn from temperature-jump relaxation measurements on cytosine and 3-methylcytosine in aqueous solutions (104). The same authors have concluded that in non-polar solvents the imino-oxo tautomer will probably become the most abundant tautomeric form (104).

Infrared matrix-isolation studies have been conducted on cytosine (25), and its methylated- (25,26), and deuterio-derivatives (25). From the analysis of the characteristic frequencies of the C=O, O-H, and N-H groups in these compounds, it was found that cytosine molecules exist in an equilibrium of two tautomeric forms (amino-oxo and amino-hydroxy) in inert matrices (25). Only the amino-oxo form was

found to be present for 1-methylcytosine (25,26), while 3-methylcytosine and 1-methylisocytosine exist mainly in their imino-oxo tautomeric forms (26). Amino-hydroxy forms were detected in the infrared spectra of matrix-isolated 6-methylisocytosine and N(2)-monomethylaminoisocytosine since only weak or no absorption bands were seen in the carbonyl region ($1800-1700\text{ cm}^{-1}$) but absorption from the hydroxy group was detected in the $3570-3560\text{ cm}^{-1}$ (O-H stretch) region (26).

Tautomerism of Purine Bases

Because of the multiplicity of possible forms, the tautomerism of purines offers a challenging field of investigation. The following principal types of tautomeric transformations liable to occur in the most significant group of purines, namely those of biological interest can be considered:

1. The prototropic tautomerism corresponding to the displacement of the proton among the four available ring nitrogens (see Figure 8).
2. The amino-imino tautomerism, liable to occur in aminopurines which may be illustrated in the particular case of adenine (see Figure 9).
3. The oxo-hydroxy tautomerism of oxopurines, illustrated for example by hypoxanthine (see Figure 10).

The crystal structure of purine has been obtained (105). A difference map enabled observation of the position of the

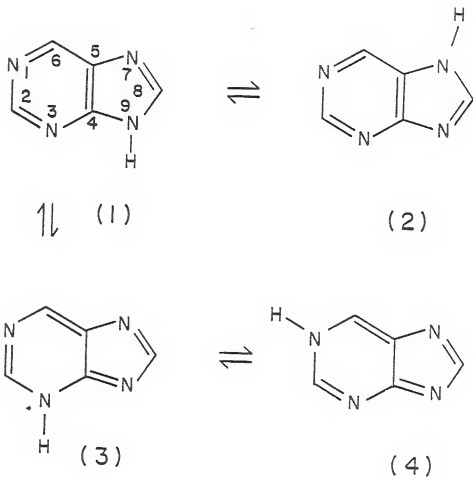


Figure 8. Tautomeric Forms of Purine.

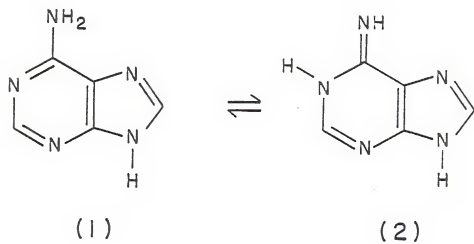


Figure 9. Amini-Imine Tautomerism in Adenine.

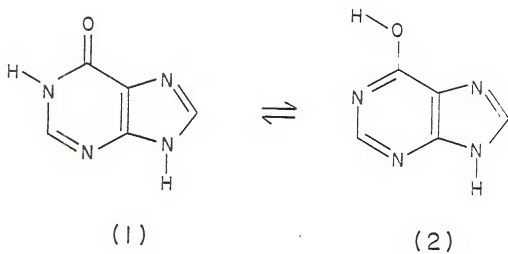


Figure 10. Oxo-Hydroxy Tautomerism in Hypoxanthine.

hydrogen atoms and in particular showed that a hydrogen is bonded to the N(7) atom.

The dipole moments of 6-methylthiopurine and of its 7- and 9-methyl- derivatives in dioxane allowed the calculation of equilibrium constants for the N(7) <--> N(9) tautomerism (106). Provided that contributions from the N(1)-H and N(3)-H and are neglected, K_T values ($K_T = [N(9)-H/N(7)-H]$) of 1.5 to 2.0 in favor of the N(9)-H tautomers, have been reported for these compounds in dioxane solutions (106). The tautomerism of all the possible mono- and bis-methylthiopurines and 2,6,8-trimethylthiopurines has also been investigated. All appeared to exist as mixtures of the N(7)-H and N(9)-H tautomeric forms based on UV, mass spectral and dipole moment evidence(107).

Comparison of the carbon-13 chemical shifts for anion formation by benzimidazole and purine in aqueous solution allowed a calculation of $K_T = [N(9)-H/N(7)-H]$ close to 1 (108). The method utilized in this calculation used the chemical shifts of the C(4) and C(5) atoms and assumed that the total effect arising from protonation of the anion is the same for benzimidazole (for which $K_T = 1.0$ as required by the symmetry) as for purine.

The infrared spectrum of isolated purine molecules in an argon matrix exhibits two strong bands in the N-H region at 3481 and 3492 cm^{-1} (25). The appearance of a doublet was

interpreted as proof of the simultaneous presence of both the N(7)-H and N(9)-H tautomeric forms in the matrix.

Many crystal structures of 9-substituted adenines confirm the 6-amino structure (109-115). Similar results were obtained from X-ray analysis of some nucleosides (116-21). These results are in agreement with the presence of absorption bands arising from NH_2 bending modes in the infrared spectra of adenines in the solid state (102,122-124).

Comparison of the ultraviolet (in aqueous solution) and infrared (KBr) spectra of 3-methyladenine to that of its N,N-dimethylamino-analogue, provided evidence of its amino structure (125). This conclusion is supported by the pK values (in 95% ethanol) of various substituted adenines (126).

A study of the basicity of analogues methylated at positions which prevented tautomerization confirmed that the amino tautomer of adenosine predominates over the imino form (127). The authors of this study attributed the increased stability of the amino forms to the greater delocalization energy of those tautomers because of the Kekule-type resonance in the pyrimidine ring.

The infrared spectrum of matrix-isolated 9-methyladenine exhibits two strong bands in the N-H region ($3600\text{--}3400\text{ cm}^{-1}$) that were assigned to the asymmetric (3557 cm^{-1}) and symmetric (3440 cm^{-1}) stretching vibrations of the amino

group (27). Three groups of doublet bands were observed in the same region for matrix-isolated adenine (27). The doublet at 3497 and 3488 cm^{-1} were assigned to the stretching vibration of the N-H group in the imidazole ring since no absorption were detected in this region in the infrared spectrum of 9-methyladenine isolated in an argon matrix (27). The band splitting was attributed to the simultaneous presence of both the N(7)-H and N(9)-H tautomers in the matrix. The splitting of the asymmetric and symmetric stretching vibrations of the amino group was also related to the simultaneous existence of both tautomers in the matrix (27). A comparison of the infrared spectrum of 9-methyladenine in the vapor phase and in CDCl_3 solutions also pointed towards the predominance of the amino tautomer (16).

Experimental evidence, mainly infrared data, has been interpreted as proof that the three isomeric, 2-, 6-, and 8-oxopurines, all exist in the solid state and chloroform solutions in the oxo form (128-130). These compounds were found to exhibit a characteristic C=O stretching vibration (near 1670 cm^{-1} in the 2- and 6-oxopurines, and near 1740 cm^{-1} in the 8-oxo isomer) but no band which could be attributed as arising from an O-H group was reported (128).

Among the polyoxopurines the attention has been centered essentially on xanthine (and some methylated derivatives). It has been reported that xanthines, in distinction to the majority of purine compounds which exist primarily as

derivatives of their N(9)-H form, exist essentially as derivatives of their N(7)-H form (131-133). The dioxo structures of xanthine (134) and theophylline (130,135) have been established by X-ray analysis. Dipole moment and ultraviolet maxima experimental data obtained from various methylxanthines, in which an extra decylthio-group was added at the 8-position to make these compounds more soluble, added proof of the predominance of the dioxo form in solution (136,137). Because of the presence of a carbonyl and an amino group, in addition to the possibility for the imidazole hydrogen to move between the N(7)- and N(9)-positions, the molecules of guanine offer numerous and complex possibilities of tautomerization (see Figure 17 in Chapter IV). In the solid state, however, only amino-oxo tautomers have been identified by X-ray analysis (138), infrared (65,102,139) and Raman spectroscopy (139).

The infrared spectra of guanine in D₂O solutions led the authors to conclude that the oxo form predominated in the oxo-hydroxy equilibria in guanine (140). The conclusion was based on the presence of a carbonyl band at 1665 cm⁻¹ in the spectra of guanine which is absent in the infrared spectra of 9-ribosyl-2-amino-6-methoxypurine. The presence of a carbonyl band does not, however, rule out the existence of other tautomeric forms in equilibrium with the oxo-tautomers. It has been shown that low-temperature spectroscopy in solidified rare gas matrices is efficient in studying

structures of isolated molecules (see section on Matrix-Isolation). Such studies have been conducted on guanine and 9-methylguanine isolated in argon (28,29) and nitrogen (28) matrices. Both studies suggested the simultaneous presence of amino-oxo and amino-hydroxy forms in the matrices. Equilibrium constant values [$K = I(OH)/I(NH)$] of 1.35 for 9-methylguanine in an argon matrix and ($K = [H]/[OH]$) 5.9 for the same compound in a nitrogen matrix have been reported (28).

CHAPTER III

EXPERIMENTAL SECTION

Matrix-Isolation: Advantages and Disadvantages

Matrix-isolation is a technique for trapping isolated molecules of the species of interest in a large excess of an inert material by rapid condensation at a low temperature so that the diluent forms a rigid matrix. If the temperature is low enough, diffusion of the solute species is prevented and thus isolated molecular complexes or reactive species may be stabilized for spectroscopic examination.

In a simple way one can think of the solute species existing as isolated molecules at low temperatures. This is so because little interaction between the "inert" matrix "cage" material (M) and the trapped solute (S) is expected. In this circumstance, the matrix environment will have a very small influence on intramolecular processes of the solute. This "cold gas model" predicts that the spectrum of the solute in low-temperature matrices will be very similar to that obtained for the free solute species (141).

Apart from the stabilization of reactive species, infrared matrix-isolation affords a number of other advantages

over more conventional spectroscopic techniques. The isolation of monomeric solute molecules in an inert environment reduces intermolecular interactions, resulting in a sharpening of the solute absorption bands as compared to other condensed phases. This effect is, of course, particularly dramatic for H-bonding substances. With the exception of a few small molecules such as HF, HCl, HBr, NH_3 , and H_2O , rotation does not occur in matrices (142). This results in much narrower bands than the vibrational-rotational bands observed in gas phase spectra. Consequently, nearly degenerate bands which overlap completely even in the vapor phase or in dilute solutions at room temperature, may often be resolved in matrix spectra. The resolution of nearly degenerate fundamentals allows the vibrational assignments to be made with greater confidence and frequencies to be obtained more accurately. Infrared matrix-isolation has also shown a great potential as a tool for studying conformational tautomerism (143), where there may be only small differences between the vibrational spectra of two conformers.

The salient features of matrix-isolation experiments are then fourfold:

1. The low concentration of the trapped species minimizes the chance of nearest-neighbor interactions.

2. The use of an inert host minimizes the perturbation of the trapped species by the environment and the resulting dispersion of energy levels.
3. The rigidity of the matrix cage inhibits diffusion of the trapped species and prevents rotation of all but the smallest molecules.
4. The low temperature minimize the thermal energy available to the trapped species thus preventing chemical dissociation and/or arrangement.

Although the matrix-isolation technique was developed to inhibit intermolecular interactions, Van Thiel, Becker, and Pimentel demonstrated its value in studying hydrogen bond interactions in H_2O (144), and CH_3OH systems (145). Bands due to monomer, dimer, trimer, and higher multimers were identified as the concentration of the solute was increased.

An understanding of the various effects that the matrix may have on the vibrational spectrum of the solute is vital to avoid misinterpretation of the spectra. The most obvious matrix effect is that the vibrational levels of the solute molecule will be perturbed by the matrix. The vibrational frequencies of the absorption bands for solutes trapped in low-temperature matrices exhibit matrix shifts, from their gas phase values, just as they exhibit solvent shifts in room temperature solution spectra; but these shifts are much

smaller (146). The same factors (electrostatic, dispersive, repulsion, and specific interactions) contribute to both (146). The high frequency stretching modes often shift to lower frequencies, while low frequency bending modes often shift to higher frequencies. The most commonly used "inert" matrix materials are the noble gases and nitrogen (since they have no absorption in the infrared) and thus normally give small frequency shifts.

Although matrix-isolation spectroscopy enables splitting of nearly degenerate bands to be observed, other small splittings may be caused by "matrix effects". Rotation or libration of the solute molecules in the matrix cage, lifting of degeneracy, aggregation, multiple trapping sites, or impurities can all cause doublet or multiplet band structure (141,146). It is thus necessary to consider carefully whether small splittings are in fact arising from tautomerism of the solute molecules. The molecules used in our study are too large to rotate under matrix conditions, thus ruling out rotation as the cause of any band splitting. Aggregation can usually be eliminated by increasing the matrix-to-solute (M/S) ratio until no further changes are observed in the spectrum. This will result in the spectrum of the monomeric species only.

Multiple site trapping effects are more troublesome since these are normally independent of the concentration of the solute. A useful diagnostic is that the additional bands

can often be removed by annealing the matrix to 35-40 K (higher temperatures may result in destruction of the matrix when argon is used as the matrix gas) for a few minutes, followed by recooling to base temperature. A more reliable way of distinguishing band splitting (due to nearly degenerate bands or isomerism) from the multiple trapping sites effects is to vary the matrix material (141,146). It is extremely unlikely that similar alternative trapping sites could exist in each of these matrix materials.

It is well known that the presence of nitrogen impurities in argon matrices may lead to the appearance of additional bands in the spectra of a variety of solutes (141,143,146-149). The stronger solute-matrix interaction and lower symmetry site of the nitrogen lattice causes modes which are degenerate in an argon matrix to be split in a nitrogen matrix.

Inactive modes of the solute may be induced by the matrix environment, for example, the hydrogen fundamental has been observed in the infrared spectrum of matrix-isolated hydrogen (150). Similarly, inactive matrix vibrations may be induced by the presence of the solute molecules. The fundamental vibration of nitrogen has been observed in the infrared spectrum of cyanogen isolated in a nitrogen matrix (151).

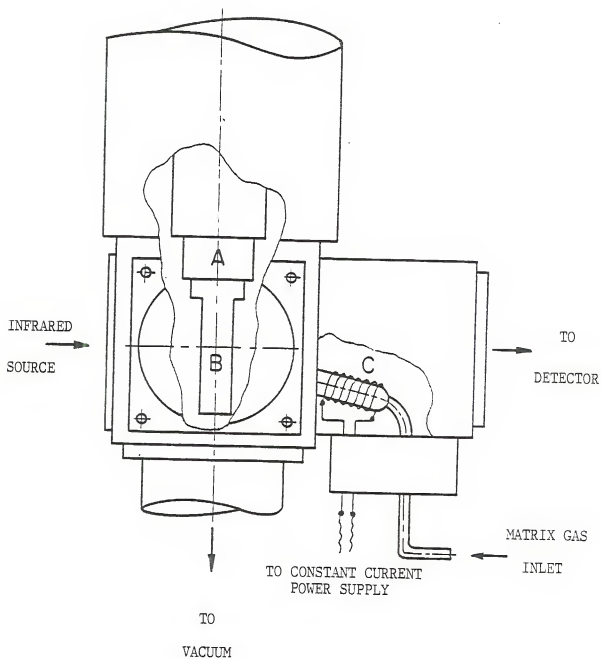


Figure 11. Vacuum Shroud and Sample Deposition Arrangement:
A=Cold Finger, B=CsI Cold Window and Window Holder,
C=Sample Container.

Preparation of Low-Temperature Samples

Infrared spectroscopy of low-temperature matrices is normally carried out using alkali halide windows in a vacuum shroud similar to that shown in Figure 11. The solid samples were contained in a resistively heated Pyrex furnace located near the cold CsI window. Enough solid to cover one third of the sample container was used in order to prevent sample splattering during the heating process. The Displex CSA 202A (Air Products and Chemicals) closed cycled helium refrigeration system was attached to the vacuum shroud and the rotary pump started (see Figure 12). Pressures of at least 10^{-2} torr were obtained (valves A, B, C, and F in Figure 12 closed) before the diffusion pump was turned on in order to prevent oxidation of the diffusion pump oil. Valve D was closed and valve F opened as soon as the diffusion pump was turned on. The trap was filled with liquid nitrogen and the pumping process allowed to continue overnight. Pressures less than 10^{-6} torr were usually attained before the temperature lowering process was started.

The compressor for the Displex CSA 202A refrigeration system was turned on and the temperature of the cold finger monitored with the temperature controller (Air Product and Chemicals). When the cold finger temperature neared 100 K, valve E (see Figure 12) was closed in order to prevent impurity backflow from the diffusion pump. The cooling process was continued for at least half an hour after the

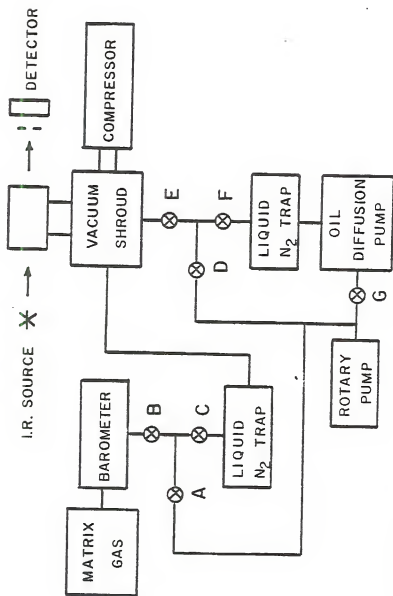


Figure 12. Schematics of Experimental Set-Up. A, B, D, E, F, and G are Low Pressure Valves and C a Needle Valve Used to Control Matrix Gas Flow.

base temperature (usually between 10-20 K) was attained in order not only to ensure temperature homogeneity of the cold window, but also to remove impurities from the system. Since water can interact with guest monomers (through hydrogen bonding), care was taken on reducing and controlling its presence in all matrices investigated. Experimental evidence indicated that water came mainly from the internal metal (stainless steel) walls of the system under vacuum on which its polar molecules are strongly absorbed. The experimental evidence consisted of

1. The absence of CO_2 absorptions in the infrared spectra of the isolated molecules indicated that water did not come in through an air leakage in the system.
2. The amount of deposited water increased with deposition time, but not with the flow rate of the matrix gas.
3. Bands due to associated water increased in intensity even in the absence of sample deposition.

Another possible source of impurities is the solid sample itself (see Table II for experimental parameters and source of the compounds studied). Since all solids were used without further purification, some impurities (mainly water) could be deposited along with the gas mixture. To minimize impurities in the final matrix, solid samples were subjected

TABLE II

Experimental Data and Source of the Compounds Under Study

COMPOUND	CURRENT (AMPERES)	DEPOSITION TEMPERATURE (°K)	DEPOSITION TIME (HRS)	SOURCE
G	1.00-1.20	10-20	1-4	SIGMA
9EG	0.90-1.00	10-20	2-6	SIGMA
DMAG	0.50-0.65	10-20	2-5	SIGMA
7MG	0.35-0.45	10-20	2-5	SIGMA
DMG	0.30-0.35	10-20	2-6	SIGMA

to high vacuum sublimation prior to deposition. This was accomplished by heating the samples (inside the vacuum shroud) to a lower temperature than that required for deposition for 15 to 30 minutes. Continuous monitoring of the cold window during this interval allowed the determination of the time at which the deposition could be started (i.e., no impurities were detected in the infrared spectrum of the cold CsI window). The heating unit was turned off and the sample allowed to cool.

In order to test for sample decomposition during the heating process; thin solid films were deposited (under the same experimental conditions used for the matrices) and their spectra recorded (see Appendix A). These same films were annealed to room temperature, cooled down to base temperature and their spectra recorded again. These spectra were compared to those obtained from KBr pellets of the same compounds (see Appendix A). Such a comparison is depicted in Figure 13 for 9-ethylguanine. The infrared spectra of the amorphous film (10 K) were found to resemble those obtained from concentrated matrices; while those of the annealed films (room temperature) resemble those obtained from KBr pellets. No sign of decomposition was detected through spectroscopic and visual examination of the samples.

The gas mixture was passed through a coil in a liquid nitrogen trap before deposition and introduced through a separate inlet. The matrix gas flow was initiated prior to

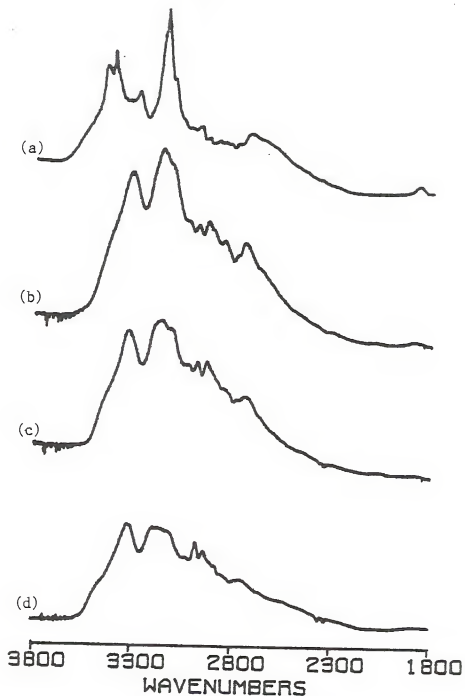


Figure 13. Infrared Spectra of 9-ethylguanine in the Solid State in the 3800-1800 and 1800-1400 Wavenumber Regions. (a) Crystalline Solid (KBr Pellets), Thin Film Annealed to Room Temperature and Recooled to Base Temperature (10°K), (c) Thin Film at Room Temperature, (d) Disordered Film at 10°K.

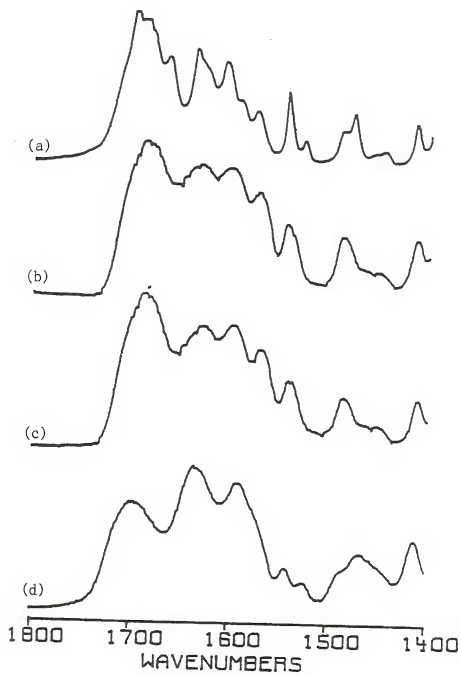


Figure 13.--continued

turning the furnace heater on and continued for several minutes after the heater had been turned off. The matrix concentration was varied by changing the flow rate of the matrix gas (needle valve C in Figure 12) at a given furnace temperature (current reported in Table II), or by changing this latter parameter at a given flow rate. In both cases, the limiting factor in obtaining sufficiently dilute matrices was matrix scattering which prevents guest absorption from being observed distinctly, especially the low intensity bands in the high frequency region of the spectrum.

The gas mixture was condensed on a CsI window (see Figure 11) maintained at the required low temperature (usually 10-20 K) by a Displex CSA 202A closed cycle helium refrigeration system. The time required to deposit sufficient sample for spectroscopic examination varied from one to six hours. Since the properties of the cold surface on which successive layers of matrix material are deposited change during deposition, matrix inhomogeneity can be expected. In order to avoid consequent nearest-neighbor interactions between sample molecules in the matrix, the total amount of guest molecules in the matrix was always kept low. This was accomplished by ending the deposition (by turning the furnace heater off) when the absorbance in the more intense region of the spectrum ($1750\text{-}1700\text{ cm}^{-1}$) was usually less than 1.0.

Materials and Equipment

Table II summarizes some experimental parameters and the source from which the organic molecules used in this study were obtained. Other inorganic compounds and their source were

1. Matrix gases (nitrogen and argon) obtained from Matheson of the highest purity available.
2. Transmission windows (KCl and KBr) as well as the deposition (CsI) windows purchased from Wilmad Company.
3. Potassium bromide used for the KBr pellets obtained from Fischer Scientific Company of spectral quality.

A schematic of the experimental set-up is shown in Figure 12. The Displex CSA 202A closed cycle helium refrigeration system (Air Products and Chemicals) consisted of the compressor, flexible lines, temperature controller, vacuum shroud and the Displex. Temperatures of 10 K could be obtained with this apparatus. The vacuum equipment consisted of an oil diffusion pump (Varian) backed by a rotary pump (Alcatel Vacuum Products, Inc. Model 410-10-304-21). Vacuum pressures were measured with an ionization gauge controller (Granville Phillips, Model 270). The current applied to the solid samples was measured with a multimeter obtained from Keithley. A constant-current power supply was built in our

laboratory by Dr. Marian Szczesniak and used to provide the current needed by the furnace.

Infrared absorption spectra were obtained with a Nicolet 7199 FT-IR spectrometer interfaced to a 1180 computer. Between 700-1,000 coadded scans were taken for the matrix-isolated samples at a 1 cm^{-1} resolution and ratioed to 200-300 coadded scans taken for the background. Infrared absorption spectra of the amorphous solid samples deposited at 10 K, their annealed films (to room temperature) and of crystalline (KBr) solid were obtained at 4 cm^{-1} resolution.

CHAPTER IV

RESULTS AND DISCUSSION

Infrared Spectra of Matrix-Isolated Guanine and Derivatives

Infrared absorption spectra of guanine (G), 9-ethyl-guanine (9EG), 2-N,N-dimethylaminoguanine (DMAG), 7-methyl-guanine (7MG), and 1,7-dimethylguanine (DMG) isolated in argon and nitrogen matrices in the 3900-700 cm^{-1} region are shown in Appendix A. Some of the possible tautomeric forms of these compounds are shown in Figures 14 to 18.

Tables III to VII summarize the observed frequencies of isolated samples of guanine and its derivatives in argon and nitrogen matrices. Included in these tables are the observed frequencies for amorphous films of these compounds deposited at 10 K, as well as those obtained from KBr pellets (infrared survey spectra in the 3900-700 cm^{-1} included in Appendix A). The assignment of the experimental absorption bands in Tables III to VII is based upon the comparison of the spectra of matrix-isolated G with that of its derivatives and with the infrared spectra of matrix-isolated pyrimidines (13-26), and purines (25,27-29), as well as upon the characteristic frequencies for the N-H, O-H, and CH₃ groups. The assignment

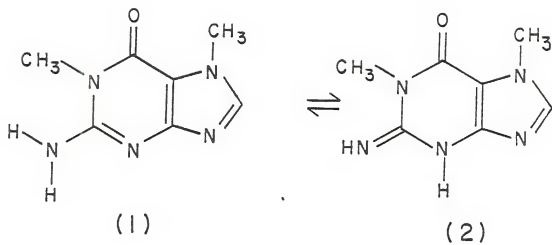


Figure 14. Tautomeric Forms of 1,7-dimethylguanine.

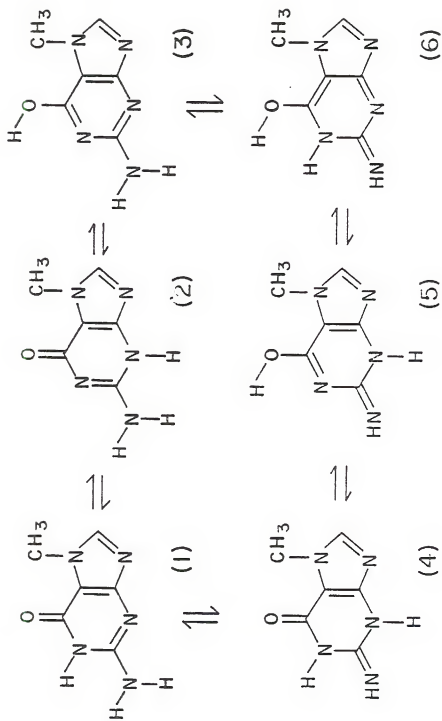


Figure 15. Tautomeric Forms of 7-methylguanine.

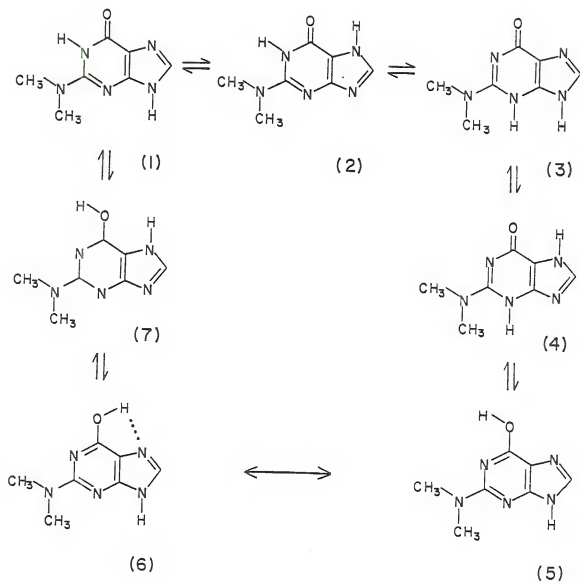


Figure 16. Tautomeric Forms of 2-N,N-dimethylaminoguanine.

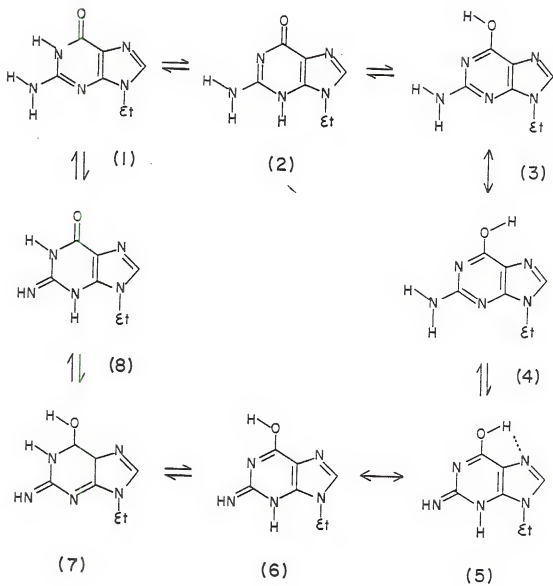


Figure 17. Tautomeric Forms of 9-ethylguanine.

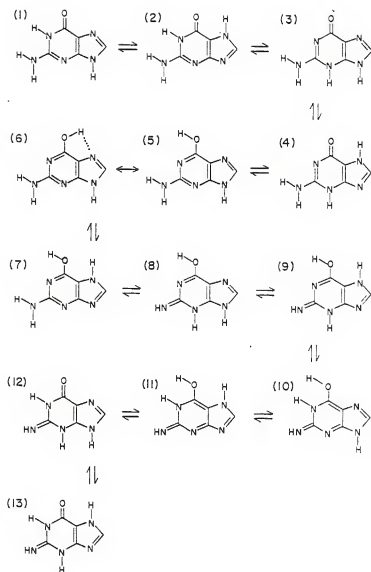


Figure 18. Tautomeric Forms of Guanine.

TABLE III

Frequencies and Assignments of the Bands in the Infrared Spectra of 1,7-dimethylguanine in Argon and Nitrogen Matrices, Amorphous Solid at 10°K and KBr Pellets.

ARGON MATRIX		NITROGEN MATRIX		SOLID FILM (10°K)		SOLID (in KBr)	
Frequency ^a (cm ⁻¹)	Assignment ^b	Frequency (cm ⁻¹)	Assignment	Frequency (cm ⁻¹)	Assignment	Frequency (cm ⁻¹)	Assignment
3530 w	NH ₂ asym str	3522 m	NH ₂ asym str			3460	NH ₂ asym str,
3428 w	NH ₂ sym str	3423 m	NH ₂ sym str			3435	
						3380	NH ₂ sym str,
				3338	NH ₂ asym str,		
				3225	NH ₂ sym str,	3200	CH ₃ str
1738 m				2940	CH ₃ str	2964	
1708 vs	C=O str					1710 sh	
1691 sh		1704 vs	C=O str				
1653 vw	ring str	1650 sh	ring str	1695 vs	C-O str	1690 vs	C=O str,
				1638 s	ring str,	1652 s	ring str,
		1618 vs	NH ₂ sc		NH ₂ sc	1634 sh	NH ₂ sc
1612 s	NH ₂ sc						

TABLE III-continued.

ARGON MATRIX		NITROGEN MATRIX		SOLID FILM (10°)		SOLID (in KBr)	
Frequency (cm ⁻¹)	Assignment	Frequency (cm ⁻¹)	Assignment	Frequency (cm ⁻¹)	Assignment	Frequency (cm ⁻¹)	Assignment
1570 m	ring str.	1568 vs	ring str.	1562 vs	ring str.		
1560 sh	CH ₃ bend	1563 vs	CH ₃ bend			1531 sh	ring str.
1554 m		1557 sh				1524 s	CH ₃ bend
1518 s		1520 vs		1525 vs	CH ₃ bend		
1496 vw	ring str.	1500 w	ring str.	1499 vw	ring str.		
1482 vw	CH ₃ bend	1485 w	CH ₃ bend	1485 vw	CH ₃ bend		
1472 sh		1475 w					
1467 vw	ring str.	1465 w		1463 w	ring str.		
1450 vw		1453 w				1458 w	ring str.
1430 m		1442 w					
1426 m		1431 sh					
1414 s	ring str.	1426 m	ring str.	1425 sh	ring str.	1424 m	ring str.
1395 m	CH ₃ bend	1395 m	CH ₃ bend	1414 s	CH ₃ bend	1414 sh	CH ₃ bend
1388 sh		1390 sh					
1355 m		1356 s		1386 m		1386 m	
1242 m		1270 vw	ring str.	1353 m		1356 m	
		1243 m		1258 vw	ring str.	1264 w	ring str.
				1245 w		1242 w	
1213 m	ring str.	1216 s	ring str.	1217 m		1222 m	
1190 m	CH ₃ bend	1190 s	CH ₃ bend				
		1130 w	ring str.	1187 w	ring str.	1182 w	ring str.
			C(8)-H bend	1130 w	C(8)-H bend	1133 w	C(8)-H bend
1123 w	ring str.						
	C(8)-H bend						

TABLE III-continued.

ARGON MATRIX			NITROGEN MATRIX			SOLID FILM (10°K)			SOLID (in KBr)		
Frequency (cm ⁻¹)	Assignment		Frequency (cm ⁻¹)	Assignment		Frequency (cm ⁻¹)	Assignment		Frequency (cm ⁻¹)	Assignment	
1062 w	ring str, NH ₂ rock		1065 w	ring str, NH ₂ rock		1101 w	ring str, NH ₂ rock		1072 w	ring str, NH ₂ rock	
			1000 m	ring str, CH ₃ bend		1067 w	ring str, CH ₃ bend		1006 w	ring str, CH ₃ bend	
994 m	ring str, CH ₃ bend					1006 m					
923 vw	ring bend		924 vw	ring bend			ring bend				
			860 vw	ring bend (out of plane)					908 vw	ring bend	
848 w	ring bend (out of plane)										
810 vw			812 vw								
781 m	ring bend		782 m	ring bend		~818 vw			782 m	ring bend	
						~778 m	ring bend				

^a Instead of intensities only approximate characteristics in terms of: vs, very strong; s, strong; m, medium; w, weak; vw, very weak; sh, shoulder are given. Abbreviation: asym, asymmetric; sym, symmetric, str, stretching; bend, bending; rock, rocking; sc, scissoring.

TABLE IV

Frequencies and Assignments of the Bands in the Infrared Spectra of 7-methylguanine in Argon and Nitrogen Matrices, Amorphous Solid at 10°K and KBr Pellets.

ARGON MATRIX		NITROGEN MATRIX		SOLID FILM (10°K)		SOLID (in KBr)	
Frequency ^a (cm ⁻¹)	Assignment ^b	Frequency (cm ⁻¹)	Assignment	Frequency (cm ⁻¹)	Assignment	Frequency (cm ⁻¹)	Assignment
3520 w	NH ₂ asym str	3516 w	NH ₂ asym str				
3436 m	N(1)-H sym str	3429 s	N(1)H sym str, NH ₂ sym str				
3420 w	NH ₂ sym str						
				3320	NH ₂ asym str,	3325	NH ₂ asym str,
				3172	N(1)-H sym str,		N(1)-H sym str,
				3112	NH ₂ sym str,	3164	NH ₂ sym str,
				2925	CH ₃ str	2875	CH ₃ str
				2770		2720	
1799 vw		1800 vw					
1767 vw							
1732 sh							
1722 vs	C=O str	1716 vs	C=O str	1695 s	C=O str		
						1685 vs	C=O str
1637 sh	NH ₂ sc bend	1640 sh	NH ₂ sc bend			1670 sh	ring str
1628 vs	ring str, NH ₂ sc	1630 vs	NH ₂ sc, ring str	1640 s	NH ₂ sc bend, ring str		
						1617 m	NH ₂ sc
				1607 sh	ring str		

TABLE IV-continued.

ARCON MATRIX		NITROGEN MATRIX		SOLID FILM (10°K)		SOLID (in KBr)	
Frequency (cm ⁻¹)	Assignment	Frequency (cm ⁻¹)	Assignment	Frequency (cm ⁻¹)	Assignment	Frequency (cm ⁻¹)	Assignment
1590 vs	ring str	1597 w	ring str				
1586 vs		1592 w					
1561 vs		1563 vs				1560 w 1569 sh	ring str, CH ₃ bend
1546 w	ring str	1543 m	ring str	1543 m	ring str		
1537 w		1537 m				1533 vs	
1500 vs		1509 vs					
1492 w	ring str, C(8)-H bend	1482 w	ring str, C(8)-H bend	1485 m	ring str, C(8)-H bend	1487 m	ring str, C(8)-H bend
1463 w		1465 w		1465 m			
1441 vs		1443 vs		1429 w		1441 vs	
1427 m		1426 m		1412 w			
1413 s		1413 s					
1389 s	ring str, CH ₃ bend	1388 s	ring str, CH ₃ bend	1384 m	ring str, CH ₃ bend	1395 m	ring str, CH ₃ bend
1355 m		1356 s					
1353 sh		1333 vs		1353 m		1358 w	
1314 vs	ring str, N(1)-H bend	1317 vs	ring str, N(1)-H bend				
		1305 w		1275 w	ring str, N(1)-H bend		ring str, N(1)-H bend
1271 w		1271 m				1270 w	

TABLE IV—continued.

ARGON MATRIX		NITROGEN MATRIX		SOLID FILM (10°K)		SOLID (In KBr)	
Frequency	Assignment	Frequency	Assignment	Frequency	Assignment	Frequency	Assignment
1232 w		1228 sh	ring str, CH ₃ bend	1223 m	ring str, CH ₃ bend	1224 m	ring str, CH ₃ bend
1225 sh	ring str, CH ₃ bend	1220 m					
1208 w		1208 w	ring str				
1186 w				1150 w	ring str, C(8)-H bend		
1145 w	ring str, C(8)-H bend	1146 w	ring str, C(8)-H bend				
1132 w		1132 w	ring str, C=O bend	1105 w	ring str, C=O bend	1110 w	ring str, C=O bend
1110 w	ring str, C=O bend	1112 w				1075 w	
1097 w				1067 w	ring str, NH ₂ rock		ring str, NH ₂ rock
1058 w	ring str, NH ₂ rock	1062 w		1045 w		1045 w	
1016 w	ring str	1021 w	ring str				
868 w		855 w	ring bend	890 w		892 w	ring bend
846 w	ring bend	846 w		850 w	ring bend	857 w	
781 m	ring bend	782 m	ring bend	780 w	ring bend	778 m	ring bend

^aInfrared of intensities only approximate characteristics in terms of: vs, very strong; s, strong; m, medium; w, weak; vw, very weak; sh, shoulder are given. Abbreviations: asym, asymmetric; sym, symmetric; str, stretching; bend, bending; sc, scissors; rock, rocking.

TABLE V

Frequencies and Assignments of the Bands in the Infrared Spectra of 2-N,N-dimethylaminoguanine in Argon and Nitrogen Matrices, Amorphous Solid at 10°K and KBr Pellets.

ARGON MATRIX		NITROGEN MATRIX		SOLID FILM (10°K)		SOLID (in KBr)	
Frequency (cm^{-1})	Assignment ^a	Frequency (cm^{-1})	Assignment	Frequency (cm^{-1})	Assignment	Frequency (cm^{-1})	Assignment
3573 w	O-H str (H)	3563 w	O-H str (H)				
3568 w		3550 w					
3507 w	N(9)-H str,						
3493 m	N(7)-H str	3486 m	N(9)-H str,				
3484 sh		3478 m	N(7)-H str				
		3454 m					
3447 m	N(1)-H str	3439 m	N(1)-H str				
		3436 sh					
1742 s				3115	O-H str,	3425	O-H str,
1723 s				2966	CH ₃ str,	3200	CH ₃ str,
1728 sh				2890	N(9)-H str,	3112	N(9)-H str,
	C=O str (O)	1736 s	C=O str (O)	2818	N(7)-H str,	2920	N(7)-H str,
					N(1)-H str	2820	N(1)-H str
1709 sh							
1701 w							
1654 m	ring str (H)	1652 sh	ring str (H)	1690 vs	C=O str	1697 vs	C=O str
		1648 m					

TABLE V-Continued.

ARGON MATRIX		NITROGEN MATRIX		SOLID FILM (10°K)		SOLID (in KBr)	
Frequency (cm ⁻¹)	Assignment	Frequency (cm ⁻¹)	Assignment	Frequency (cm ⁻¹)	Assignment	Frequency (cm ⁻¹)	Assignment
1624 w	ring str (O)	1619 w	ring str (O)			1624 vs	ring str (O)
		1605 sh					
1600 vs	ring str (H)	1600 vs	ring str (H)	1600 vs	ring str (H)	1607 vs	ring str (H)
1594 vs		1592 vs					
		1585 sh					
		1578 m	ring str (O), CH ₃ bend				
1570 m	ring str (O), CH ₃ bend						
1552 sh		1547 m	ring str,				
1550 m	ring str,	1537 sh	CH ₃ bend	1550 s	ring str, CH ₃ bend	1535 sh	ring str, CH ₃ bend
1539 sh	CH ₃ bend	1454 w				1452 w	
1450 w		1448 w	ring str,	1447 m	ring str, O-H bend (H)		
1437 w	ring str,	1439 w	O-H bend (H)				
1429 w	O-H bend (H)						
1409 sh		1410 w	ring str,				
1404 m	ring str,	1403 w	CH ₃ bend				
1395 w	CH ₃ bend	1395 w				1402 vw	
				1383 s	ring str,		
1372 m	ring str,	1372 m	ring str,				
	N(9)-H str,	1344 m	N(9)-H str,	1345 s	ring str, N(9)-H str	1371 m	
1340 m	N(7)-H str					1348 m	
		1335 sh	N(7)-H str			1335 sh	
1327 vw							

TABLE V-continued.

ARGON MATRIX		NITROGEN MATRIX		SOLID FILM (10°K)		SOLID (in KBr)	
Frequency (cm ⁻¹)	Assignment	Frequency (cm ⁻¹)	Assignment	Frequency (cm ⁻¹)	Assignment	Frequency (cm ⁻¹)	Assignment
1301 w	ring str	1293 w	ring str	1293 w	ring str	1295 w	ring str
		1281 vw	ring str,				
		1274 w	N(1)-H bend				
1270 w	ring str,						
	N(1)-H bond						
1254 w	ring str,	1256 w	ring str,	1247 w	ring str, (II)	1260 vw	ring str,
1248 w	O-H bend (II)		O-H bend (II)		O-H bend (II)	1245 w	O-H bend (II)
				1216 m	ring str,		
					CH ₃ bend		
1201 w	ring str,	1205 sh	ring str,				
	CH ₃ bend	1202 w	CH ₃ bend				
1162 w	ring str,			1187 m	ring str,	1165 vw	ring str
1143 w	O-H bend (II)	1160 w	ring str,		O-H bend (II)	1145 sh	
		1140 w	O-H bend (II)	1140 m			
		1134 vw					
1113 m	ring str,	1117 w	ring str,	1115 m	ring str,	1130 w	ring str,
	C=O bend (O)	1110 sh	C=O bend (O)		C=O bend (O)	1113 w	C=O bend (O)
1070 w	ring str	1071 w	ring str	1070 w	ring str	1075 w	ring str
		1066 w					
1053 vw							
1033 w	ring str,	1038 sh	ring str,				
1025 w	O-H bend (II)	1027 w	O-H bend (II)	1032 m	ring str,	1040 vw	ring str
989 vw	ring bend,				O-H bend (II)		
	C=O bend (O)						

TABLE V-continued.

ARCON MATRIX			NITROGEN MATRIX			SOLID FILM (10°K)			SOLID (in KBr)		
Frequency (cm ⁻¹)	Assignment		Frequency (cm ⁻¹)	Assignment		Frequency (cm ⁻¹)	Assignment		Frequency (cm ⁻¹)	Assignment	
934 vw	C-O bend (H),		938 vw	C-O bend (H),		945 sh	C-O bend (H),		946 w	C-O bend (H)	
908 w	ring bend		931 w	ring bend		973 w	ring bend			ring bend	
	(out of plane)		908 w	(out of plane)		908 w	(out of plane)		910 w	(out of plane)	
898 vw	ring bend										
853 vw	(out of plane)										
793 w	ring bend (H)		793 vw	ring bend (H)		790 sh	ring bend (H)		791 w	ring bend (H)	
781 w	ring bend (O)		781 w	ring bend (O)		780 m	ring bend (O)		778 w	ring bend (O)	

^a Instead of intensities only approximate characteristics in terms of: vs, very strong; s, strong; m, medium; w, weak; vw, very weak; sh, shoulder.
 Abbreviations: asym, asymmetric; sym, symmetric; str, stretching; bend, bending; sc, scissors; rock, rocking; (H), hydroxy tautomer; (O), oxo tautomer.

TABLE VI
Frequencies and Assignment of the Bands in the Infrared Spectra of 9-ethylguanine in Argon and Nitrogen Matrices, Amorphous Solid at 10°K and KBr Pellets.

ARGON MATRIX		NITROGEN MATRIX		SOLID FILM (10°K)		SOLID (in KBr)	
Frequency ^a (cm ⁻¹)	Assignment ^b	Frequency (cm ⁻¹)	Assignment	Frequency (cm ⁻¹)	Assignment	Frequency (cm ⁻¹)	Assignment
3569 m	O-H str (H)	3567 sh	O-H str (H)				
3567 sh		3563 m					
		3555 sh					
		3550 m					
3534 w	NH ₂ asym str	3535 w	NH ₂ asym str	3450		3450	
3452 m	N(1)-H str	3453 m	N(1)-H str				
3435 m	NH ₂ sym str (H)	3436 m	NH ₂ sym str (H)				
3430 sh	NH ₂ sym str (O)	3422 m	NH ₂ sym str (O)				
				3320	O-H str, NH ₂ asym str,	3414	O-H str, NH ₂ asym str,
				3190	NH ₂ sym str,	3286	NH ₂ sym str,
				3110	N(1)-H str,	3148	N(1)-H str,
				2960	CH ₃ str	3110	
				2935		2970	CH ₃ str
1779 vw	C=O str					2930	
1745 s		1742 sh				2720	
1723 w		1734 s	C=O str	1695 s	C=O str	1698 vs	C=O str
						1687 sh	

TABLE VI—continued.

ARGON MATRIX		NITROGEN MATRIX		SOLID FILM (10°K)		SOLID (in KBr)	
Frequency (cm ⁻¹)	Assignment	Frequency (cm ⁻¹)	Assignment	Frequency (cm ⁻¹)	Assignment	Frequency (cm ⁻¹)	Assignment
1644 s	ring str (H)	1643 s	ring str (H)			1665 sh	ring str,
1636 sh	ring str (O)	1636 sh	ring str (O)			1643 vs	NH ₂ sc
1624 vs	NH ₂ sc,	1627 vs	NH ₂ sc	1631 vs	ring str,		
	ring str				NH ₂ sc		
1620 s							
1608 w		1602 m				1608 vs	ring str (H)
1600 sh		1597 s					
1593 s		1591 s	ring str (H)	1590 s	ring str (H)	1593 sh	
1590 vs	ring str (H)	1588 sh					
1582 m						1576 sh	
1562 m	ring str (O)	1564 s	ring str (O)				
	CH ₃ bend	1558 w		1542 w	ring str	1545 s	ring str (O)
1536 w						1527 w	
1521 w	ring str,	1520 w	ring str,	1520 w	ring str,		
	CH ₃ bend		CH ₃ bend		CH ₃ bend		
1489 vw	ring str,	1490 w	ring str,	1489 w	ring str,	1488 sh	ring str,
1485 vw	C(8)-H bend		C(8)-H bend	1485 vw	C(8)-H bend		C(8)-H bend,
1476 vw		1477 w	ring str,		ring str,	1478 s	CH ₃ bend
1467 m	CH ₃ bend	1469 m	CH ₃ bend	1467 m	ring str,		
					CH ₃ bend		
1459 vw		1457 vw	ring str,			1456 sh	ring str,
1456 w	O-H bend	1448 w	O-H bend			1447 w	O-H bend
1446 w							

TABLE VI-continued.

ARGON MATRIX		NITROGEN MATRIX		SOLID FILM (10°K)		SOLID (In KBr)	
Frequency (cm ⁻¹)	Assignment	Frequency (cm ⁻¹)	Assignment	Frequency (cm ⁻¹)	Assignment	Frequency (cm ⁻¹)	Assignment
1439 m	ring str, O-H bend, CH ₃ bend	1441 w	ring str, O-H bend, CH ₃ bend	1412 m	ring str, O-H bend, CH ₃ bend	1415 m	ring str, O-H bend, CH ₃ bend
1428 sh		1427 sh				1395 s	
1424 s		1424 m				1380 s	
1419 m		1418 s				1353 w	
1412 sh							
1399 w		1398 w					
1386 w							
1370 vw	ring str, N(1)-H bend	1377 vw	ring str, N(1)-H bend	1358 w			
1362 w		1369 w					
1358 w		1364 w					
		1359 vw					
		1331 vw					
1316 vw	ring str, N(1)-H bend	1317 m	ring str, N(1)-H bend				ring str, N(1)-H bend
1287 vw						1313 w	
1277 w		1282 vw	ring str			1304 w	
		1277 w					
1251 vw		1256 vw					
	ring str, O-H bend	1247 w	ring str, O-H bend	1242 w	ring str, O-H bend		ring str, O-H bend, CH ₃ bend
1240 w		1243 w				1235 sh	
1233 w		1232 vw				1224 w	
1220 m	ring str, CH ₃ bend	1215 w	ring str, CH ₃ bend	1219 vw	ring str	1215 sh	
1217 sh							

TABLE VII

Frequencies and Assignments of the Bands in the Infrared Spectra of Guanine in Argon and Nitrogen Matrices, Amorphous Solid at 10°K and KBr Pellets.

ARGON MATRIX		NITROGEN MATRIX		SOLID FILM (10°K)		SOLID (in KBr)	
Frequency ^a (cm ⁻¹)	Assignment ^b	Frequency (cm ⁻¹)	Assignment	Frequency (cm ⁻¹)	Assignment	Frequency (cm ⁻¹)	Assignment
3576 sh							
3571 m	O-H str (H)	3570 w					
3563 sh		3564 m	O-H str (H)				
3543 sh		3550 sh					
3538 w	NH ₂ asym str (H)						
3528 sh		3530 vw					
3525 w	NH ₂ asym str (O)						
3497 m			NH ₂ asym str (H)				
3493 m	N(9)-H str,						
3489 m	N(7)-H str						
3483 s							
3473 w		3447 m					
3458 sh		3462 m	N(9)-H str,				
3456 m		3472 s	N(7)-H str				
3437 s							
		3456 m	N(1)-H str				
			NH ₂ asym str (H)				
3433 sh		3436 sh					
3431 sh							
3426 m							
			NH ₂ asym str (O)				
		3424 s					
			NH ₂ -sym str (O)				

TABLE VII-continued.

ARGON MATRIX		NITROGEN MATRIX		SOLID FILM (10°g)		SOLID (in KBr)	
Frequency (cm ⁻¹)	Assignment	Frequency (cm ⁻¹)	Assignment	Frequency (cm ⁻¹)	Assignment	Frequency (cm ⁻¹)	Assignment
1752 sh	C=O str			3310	NH ₂ asym str,	3340	
1748 s	[N(9)-H taut.]	1744 s	C=O str		NH ₂ sym str,	3135	NH ₂ asym str,
1736 s	C=O str		[N(9)-H taut.]	3110	NH ₂ sym str,	3118	NH ₂ sym str,
1732 sh	[N(7)-H taut.]	1729 vs	C=O str	3000	N(9)-H str,		N(9)-H str,
1718 w		1714 m	[N(7)-H taut.]	2900	N(7)-H str,	2990	N(7)-H str,
1704 w				2820	N(1)-H str	2910	N(1)-H str,
						2850	N(1)-H str
						2780	
						2700	
1654 m	ring str (II)	1654 m	ring str (II)	1690 vs	C=O str,	1698 vs	C=O str,
1652 sh		1650 sh			ring str		ring str,
1628 vs		1629 vs	* NH ₂ sc	1632 vs	ring str,	1675 vs	NH ₂ sc
1619 s	NH ₂ sc					1635 w	ring str
1608 w							
1601 m	ring str (II)						

TABLE VII—continued.

ARGON MATRIX		NITROGEN MATRIX		SOLID FILM (10°K)		SOLID (in KBr)	
Frequency (cm ⁻¹)	Assignment	Frequency (cm ⁻¹)	Assignment	Frequency (cm ⁻¹)	Assignment	Frequency (cm ⁻¹)	Assignment
1593 vs		1597 m	ring str (H)	1593 vs	ring str (H)		
1587 sh	ring str (H)	1593 m					
1582 sh							
1575 s	ring str (O)	1578 s	ring str (O)				
1565 w	ring str					1565 m	ring str
1562 w							
1552 m		1547 m					
1546 m	ring str						
		1540 m	ring str				
1531 w		1534 w	ring str				
1506 m		1508 w					
1483 v	ring str, C(8)-H bend	1466 vs	ring str, C(8)-H bend				
1472 m		1475 m					
1455 vs		1456 w		1460 m	ring str, C(8)-H bend	1477 m	ring str, C(8)-H bend
1452 v						1463 sh	
1448 vs	ring str, O-H bend (H)	1445 w	ring str, O-H bend (H)				
1443 m		1438 w					
1432 w							
1423 sh							
1418 s	ring str	1418 m					
1404 m		1404 m	ring str			1417 w	ring str
1378 sh							
1375 s	ring str, N(9)-H bend	1376 m	N(9)-H bend,				
		1367 sh		1368 m	ring str, N(9)-H bend	1376 m	ring str, N(9)-H bend
1360 w	ring str	1356 m	ring str				
1352 m							

TABLE VII—continued.

ARGON MATRIX		NITROGEN MATRIX		SOLID FILM (10°K)		SOLID (1n KBr)	
Frequency (cm^{-1})	Assignment	Frequency (cm^{-1})	Assignment	Frequency (cm^{-1})	Assignment	Frequency (cm^{-1})	Assignment
1340 w	ring str, O-H bend (H)	1342 w	ring str, O-H bend (H)				
1329 m		1331 w					
1321 w		1316 w	ring str				
1308 w		1310 w					
1292 w	ring str,	1280 sh		1283 w			
1275 v	N(1)-H bend	1273 w	ring str, N(1)-H bend		ring str, N(1)-H bend		
1271 sh		1259 w		1262 w		1262 w	ring str, N(1)-H bend
1259 v						1217 w	ring str
1210 w	ring str, O-H bend (H)	1183 m	ring str, O-H bend (H)				
1194 w		1160 w					
1183 m		1140 w	ring str, C(8)-H bend	1154 w	ring str,	1174 w	ring str
1178 sh		1130 w				1150 sh	ring str, C(8)-H bend
1157 w						1120 w	C=O bend
1140 w	ring str, C(6)-H bend	1103 w	ring str, C=O bend	1108 w	ring str, C=O bend		
1131 w		1058 w	ring str, NH ₂ rock				
1103 w							
1063 w							
1052 w							
1049 w						1044 w	

TABLE VII-continued.

AROM MATRIX		NITROGEN MATRIX		SOLID FILM (10°K)		SOLID (in KBr)	
Frequency (cm ⁻¹)	Assignment	Frequency (cm ⁻¹)	Assignment	Frequency (cm ⁻¹)	Assignment	Frequency (cm ⁻¹)	Assignment
1026 w	ring str, O-H bend (H)						
1017 w	ring bend, C-O bend	1010 vw	ring str, O-H bend (H)				
975 w	(out of plane)		ring bend, C=O bend				
		968 w	(out of plane)				
932 w	ring bend (in plane)	931 w	ring bend (in plane)	936 w	ring bend (in plane)	950 w	ring str, C-O bend (out of plane)
925 w	ring bend (in plane)	929 w	ring bend				
			ring bend (out of plane)			880 w	
855 w	ring bend (out of plane)	864 w	ring bend (out of plane)			850 w	ring bend (out of plane)
838 w	ring str, ring bend (in plane)	837 w	ring str, ring bend (in plane)	830 w	ring str, ring bend (in plane)	840 sh	
827 w	ring bend (in plane)	822 w	ring bend (in plane)				
794 w	ring bend (H)	791 w	ring bend (H)	797 w	ring bend (H)	790 sh	ring bend
			ring bend (O)	786 w	ring bend (O)		
781 m	ring bend (O)	782 m	ring bend (O)			779 w	ring bend

^a Instead of intensities only approximate characteristics in terms of: vs, very strong; s, strong; m, medium; w, weak; wv, very weak; sh, shoulder are given. ^b Abbreviations: asym, asymmetric; sym, symmetric; str, stretching; bend, bending; rock, rocking; sc, scissoring; (H), hydroxy tautomer; (O), oxo tautomer; (O), oxo tautomer; taut., tautomer.

has to be considered only preliminary since ab initio calculations have been performed only for the amino-oxo tautomer of G (152.153), but not for the other tautomeric forms or for guanine derivatives.

The 3600-3400 cm^{-1} Region

Expanded scale spectra of this region for isolated samples in argon and nitrogen matrices are shown in Appendix B. Additionally, a comparison of the absorption spectra of all compounds studied isolated in argon matrices is depicted in Figure 19.

Ab initio calculations with a 3-21G basis set on the amino-oxo tautomeric form of G (form 1 in Figure 18) predicted two absorption bands (arising from the asymmetric and symmetric stretching modes of the amino group) to appear at 3563 and 3454 cm^{-1} , respectively (152). The fixed amino-oxo derivative of guanine, DMG, shows as expected only two absorption bands in this region at 3530 and 3428 cm^{-1} (see Figures 14 and 19). A small frequency shift (about 8 cm^{-1}) for these bands was observed in the infrared spectrum of DMG isolated in a nitrogen matrix (see Table III and Figure B.1). The band separation of about 102 cm^{-1} is smaller than that reported for the separation of the amino symmetric and asymmetric stretches in 2-aminopyridine and 1-methylcytosine of about 113-120 cm^{-1} , but close to the theoretical value of 109 cm^{-1} predicted by ab initio calculations for the amino-oxo tautomer of G (152). The observed intensity ratio

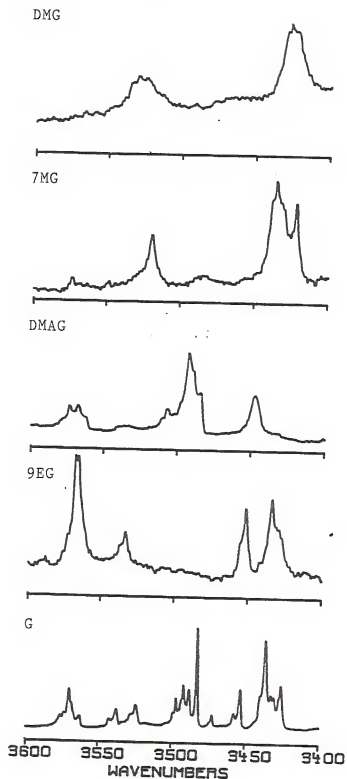


Figure 19. Infrared Spectra of Guanine and Its Derivatives in the 3600-3400 Wavenumber Region.

($A_{\text{asym}}/A_{\text{sym}} = I_{\text{asym}}/I_{\text{sym}}$) of 0.6 in DMG compares favorably with the value of 0.7 reported in studies of 2-amino pyridine and 1-methylcytosine (26,28), and with the theoretical value of 0.55 (152). Hence, these bands (3530 and 3428 cm^{-1}) are assigned to the asymmetric and symmetric stretches, respectively, of the amino group in this fixed oxo-derivative of G. Values of 3557 and 3438 cm^{-1} in 9-methyladenine and adenine (27), and 3559 and 3438 cm^{-1} in cytosine (24), respectively, have been reported for the frequencies of these two bands in infrared matrix-isolation studies of these compounds.

Three absorption bands appeared in the infrared spectrum of 7MG isolated in an argon matrix, while only two could be seen in the spectrum obtained from a nitrogen matrix (see Figure B.2). The bands at 3520 and 3420 cm^{-1} (when isolated in argon matrices) exhibited the same frequency spacing (about 100 cm^{-1}) as that shown by the asymmetric and symmetric stretches of the amino group in DMG, and are therefore assigned as arising from the same vibrational modes.

The symmetric stretch of the N(1)-H group is predicted to appear at 3445 cm^{-1} (152,153). Frequencies around 3430 cm^{-1} have been reported for the same vibrational mode (the N(1)-position in purines correspond to the N(3)-position in pyrimidines) in infrared matrix-isolation studies of

1-methyluracil (20,21) and uracil (19,22,23). The band at 3428 cm^{-1} in the spectrum of 7MG isolated in an argon matrix is then assigned to this vibrational mode. The "abnormal" high intensity of the absorption band around 3430 cm^{-1} in the spectrum of 7MG isolated in a nitrogen matrix (as compared to the spectrum obtained from an argon matrix) must be due to the overlap of the N(1)-H and amino symmetric stretches.

Three absorption bands (a doublet at 3573 and 3568 cm^{-1} and strong bands at 3493 and 3447 cm^{-1}) were seen in the infrared spectrum of 2-N,N-dimethylaminoguanine (DMAG) isolated in argon matrices. Both the amino hydrogens of DMAG have been replaced by methyl groups; hence, no absorption from the amino group is expected in this region. Infrared matrix-isolation studies on cytosine and 2-oxo-pyrimidines have reported the presence of a band around 3580 cm^{-1} which has been assigned to a stretching vibration of the O-H group (24). Similar bands have been reported for matrix-isolated 6-methylisocytosine and isocytosine (26), which have been shown to exist in the matrix mainly as their amino-hydroxy tautomeric forms. The doublet at 3573 and 3668 cm^{-1} is therefore assigned to a hydroxyl group stretching mode. The appearance of a doublet in both matrices (argon and nitrogen) rules out multiple trapping sites as the cause of the band splitting. A possible explanation for this splitting could be the simultaneous presence of tautomeric forms 5, 6 and/or 7 (in Figure 16) in

the matrices. Different frequencies have been reported by Mason for the O-H stretch in the infrared spectra of N-heteroaromatic compounds (129). A sharp band around 3600 cm^{-1} (for a free O-H) for those molecules with a hydroxyl group which was neither alpha or gamma to a ring-nitrogen atom and a broad band in the $3395\text{--}3470\text{ cm}^{-1}$ region for those molecules with a hydroxyl group peri to a ring nitrogen (due to an intramolecular hydrogen-bonded O-H stretching vibration) were reported for some of these compounds in carbon tetrachloride solutions (129). The absorption band around 3447 cm^{-1} in the infrared spectrum of DMAG isolated in an argon matrix is assigned to the N(1)-H stretching vibration. Ab initio calculations predict this frequency to appear at 3445 cm^{-1} (152,153). The better agreement (as compared to 7MG) might be due to the removal of the normal coordinate mixing between the N(1)-H and amino symmetric stretches by methylation of the amino group in DMAG.

The absorption bands in the $3520\text{--}3480\text{ cm}^{-1}$ region are present in the infrared spectra of matrix-isolated DMAG and G but not in those of 7MG, 9EG, and DMG; all of which have been methylated at the N(7)- or N(9)-positions. This observation suggests that these absorption bands arise from the N(9)-H stretching vibration, which is predicted to appear at 3503 cm^{-1} in the infrared spectrum of the amino-oxo monomer of G (152,153). The complex structure of these absorption bands also suggests that more than one vibrational

mode absorbs in this region. It seems that some contribution from the N(7)-H stretching mode from tautomeric forms 2, 4, and/or 7 of DMAG (see Figure 16), and 2, 4, and/or 7 of G (see Figure 18), may also appear here. The simultaneous presence of both the N(7)-H and N(9)-H tautomers in a matrix have been reported for purine and adenine in argon matrices (27). Frequencies around 3497 and 3488 cm^{-1} were reported for these vibrational modes in these compounds (27). The presence of at least two strong carbonyl bands in the infrared spectra of DMAG and G in nitrogen and argon matrices, while only one band is seen in the same region in the spectra of 7MG, 9EG, and DMG seems to provide further proof of the contribution of the N(7)-H symmetric stretch to these absorption bands (see section on carbonyls discussed later).

The infrared spectrum of 9EG isolated in an argon matrix shows at least four bands in this region (see Figure 19), while five bands appeared in the spectrum when nitrogen was used as the matrix gas (see Figure B.4). The bands at 3534 and 3435 cm^{-1} in the argon matrix exhibited the same frequency spacing (about 100 cm^{-1}) and are very close in frequency as the asymmetric and symmetric stretches of the amino group in DMG and 7MG, and are therefore assigned as arising from the same vibrational modes.

The strong absorption band around 3570 cm^{-1} in the argon matrix exhibited a complex structure in the nitrogen matrix, with subbands at 3572 , 3563 , and 3550 cm^{-1} (see Figure B.4). Similar subbands have been discussed earlier for the infrared absorption spectra of DMAG and were assigned to a hydroxyl group stretching mode. The splitting in the nitrogen matrix could be due to matrix splitting (see section on Matrix-isolation discussed earlier) or to the simultaneous presence of tautomeric forms 3 and 4 in the matrix (see Figure 17).

The splitting of the symmetric stretch of the amino group (3435 cm^{-1}) in the infrared spectrum of 9EG isolated in a nitrogen matrix could be explained by the stronger solute matrix interaction in nitrogen matrices (see section on matrix-isolation). Modes which are degenerate in an argon matrix are known to split in a nitrogen matrix ($141, 143, 146-149$). Therefore, the bands at 3436 and 3422 cm^{-1} are tentatively assigned to the symmetric stretch of the amino group in the amino-oxo and amino-hydroxy tautomers of 9EG, respectively. A similar splitting in this region have been reported in the infrared spectrum of cytosine isolated in a nitrogen matrix (154) and attributed to the same matrix effect. The corresponding asymmetric stretches of the amino group in 9EG are then responsible for the broad absorption seen around 3532 cm^{-1} .

The infrared spectrum of G isolated in an argon matrix shows at least eight absorption bands in this region, most of

them with complex structure or subbands. The absorption bands in the $3500\text{--}3480\text{ cm}^{-1}$ region have been assigned earlier to the symmetric stretch of the N(9)-H group with possible contributions from the N(7)-H tautomeric forms. The band at 3454 cm^{-1} is assigned to the N(1)-H symmetric stretch in good agreement with the values found for DMAG (3447 cm^{-1}) and 9EG (3452 cm^{-1}).

The splitting of the bands in the $3450\text{--}3420\text{ cm}^{-1}$ region is similar to that seen in the infrared spectrum of 9EG isolated in a nitrogen matrix discussed earlier. The absorption band at 3437 cm^{-1} is then assigned to the symmetric stretch of the amino group in the amino-oxo tautomers of G and that at 3426 cm^{-1} to the same vibrational mode in the amino-hydroxy tautomers of G (see Figure 18). The corresponding asymmetric stretches are then seen, with the usual frequency spacing of about 100 cm^{-1} , at 3538 and 3525 cm^{-1} , respectively.

The band at 3472 cm^{-1} could arise from the N(3)-H symmetric stretch of tautomeric forms 3 and 4 in Figure 18. Similar frequencies have been reported for the same vibrational mode in matrix-isolation studies of 3-methyluracil (20). Another possibility is that it arises from the N(7)-H symmetric stretch of tautomeric forms 2, 4, and/or 13 (see Figure 18). The lower frequency could be then explained by the interaction of the hydrogen atom with one of the lone pairs of the oxygen atom.

The complex structure of the absorption bands around 3570 cm^{-1} in both argon and nitrogen matrices seems to suggests the simultaneous presence of more than one hydroxy form in the matrices. These bands have been assigned to the O-H symmetric stretch through the comparison of the spectra of G to those of DMAG, 9EG, and pyrimidines (24-26,154).

The $1800\text{--}700\text{ cm}^{-1}$ Region

The interpretation of the infrared spectra of guanine and its derivatives in this region is much more difficult than that of the region previously discussed. The difficulties arise from the following:

1. The lack of reliable calculations of normal modes, frequencies and intensities for all the possible tautomeric forms of the molecules under study.
2. The possibility of Fermi resonance between the fundamentals and combination vibrations.
3. The superposition and/or splitting of the bands due to the presence of different tautomers in the matrix.

Recently, calculations of normal modes were performed for guanine, but only the amino-oxo tautomer was considered (152). The results of these calculations were taken into account in the assignment of the absorption bands. But we are aware of the fact that substitution of hydrogen by methyl groups or the probability that these compounds may be present

in more than one tautomeric form in the matrix, might influence the spectrum obtained in this region very strongly. Hence, the comparison of the experimental spectrum with the predicted one must be performed very cautiously.

Ab initio calculations on the amino-oxo tautomer of G predicted a strong absorption band at 1773 cm^{-1} arising from the carbonyl stretching mode, two absorptions from the amino scissoring (1634 cm^{-1}) and bending (1610 cm^{-1}) modes, and a strong band arising from a ring stretching vibration at 1570 cm^{-1} (152,153). The fixed amino-oxo derivative of G, DMG and 7MG exhibit very strong bands at 1708 and 1722 cm^{-1} , respectively (see Figure 20). A 5 cm^{-1} frequency shift was detected for both compounds when isolated in a nitrogen matrix (see Figures C.1 and C.2). The strong absorption band at 1745 cm^{-1} in the infrared spectrum of 9EG isolated in an argon matrix shifted to 1734 cm^{-1} when nitrogen was used as the matrix gas (see Figure C.4). These bands are assigned to the stretching mode of the carbonyl group. Similar bands have been observed in the infrared spectra of matrix-isolated uracils (17,19-23), cytosines (25,26,154), oxopyrimidines (14), and ketones (155,156); and have been assigned to the same vibrational mode (C=O stretch). The lower frequency for this band in DMG as compared to 7MG and 9EG could be a result of N(1)-methylation. A similar effect has been reported in the fixed oxo forms 4-oxo-3,6-dimethyl and 4-oxo-1,6-dimethyl-pyrimidines when isolated in argon matrices (14).

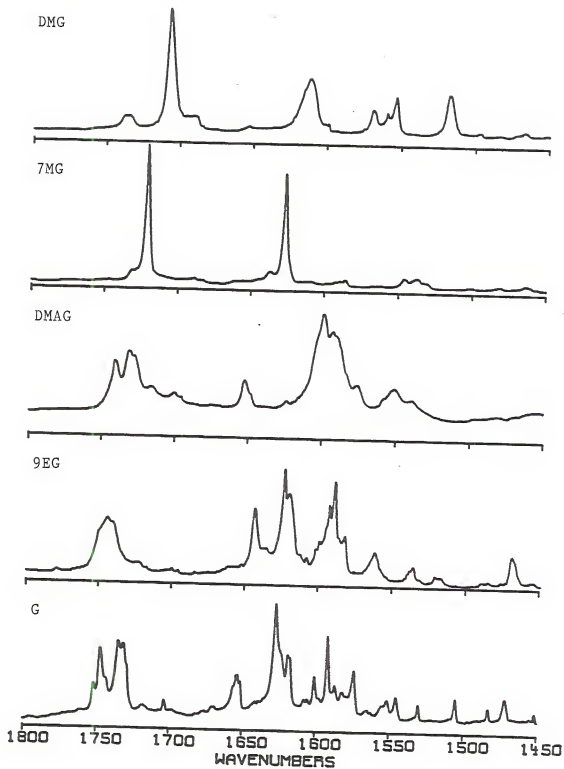


Figure 20. Infrared Spectra of Guanine and Its Derivatives in the 1800-700 Wavenumber Region.

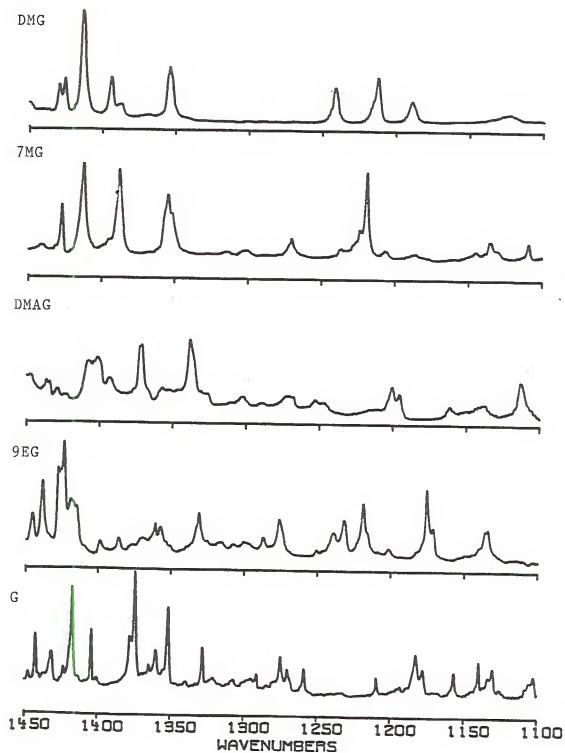


Figure 20.--continued

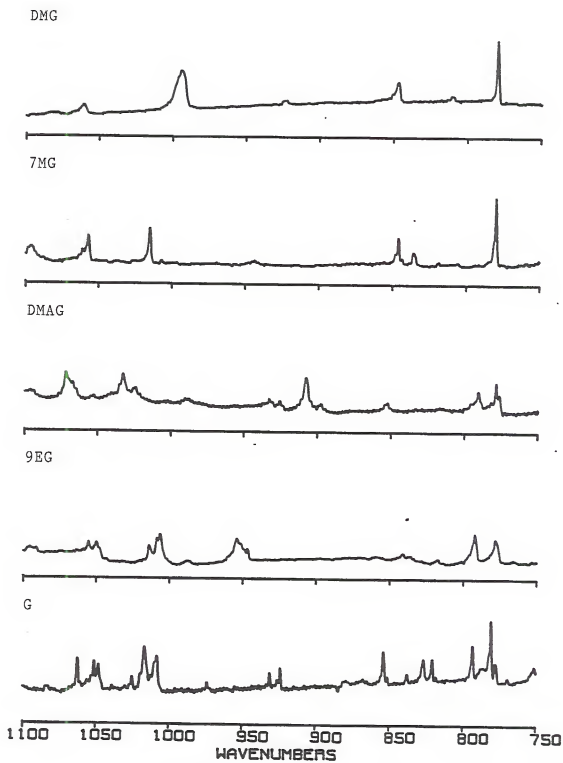


Figure 20.--continued

In contrast the infrared spectra of G and DMAG exhibited a complex structure with more than one band when isolated in both matrices (argon and nitrogen), thus ruling out multiple trapping sites as the cause of the band splitting. The splitting of carbonyl group absorption bands as well as those from other functional groups is not a phenomenon that is new to infrared spectroscopy (143). The splitting of the carbonyl band in those compounds where rotational isomerization could play a role can be sensitive to the phase (vapor, solution, or solid) as well as to aggregation of the solute molecules in the matrix (141,146,155,156). Fermi resonance is another possible explanation of this phenomenon. The absence of such a complex band structure in the spectra of 7MG and DMG points to the presence of more than one tautomeric form as the most probable explanation since this splitting is seen only (in our study) in those compounds which shown the capability of exhibiting N(9)-H and N(7)-H tautomerism. The comparison of the frequencies of these absorption bands in G and with those of 7MG and 9EG, led to the assignment of the low frequency band (1733 cm^{-1} in DMAG and 1736 cm^{-1} in G) to the carbonyl stretching vibration of the amino-oxo tautomeric forms of these compounds with the imidazole hydrogen attached to the N(7)-atom (1722 cm^{-1} in DMG), while the high frequency band (1744 cm^{-1} in DMAG and 1748 cm^{-1} in G) is assigned to the same vibrational mode of the amino-oxo tautomers with the hydrogen attached to the

N(9)-atom (1745 cm^{-1} in 9EG). A different frequency for this absorption has been reported by Mason in his infrared study of N-hetero-aromatic hydroxy (and/or oxo) compounds (129). While the carbonyl stretching mode of 6-oxo-7-methylpurine appeared at 1702 cm^{-1} in chloroform and 1697 cm^{-1} in the solid state, the same vibrational mode comes at 1711 and 1679 cm^{-1} , respectively for the same states in 6-oxo-9-methylpurine.

The strong band at 1654 cm^{-1} in G and DMAG and 1644 cm^{-1} in 9EG is not seen in the infrared spectra of matrix-isolated 7MG or DMG (see Figure 20). A band around this frequency has been assigned to the NH_2 scissoring mode in adenine and 9-methyladenine isolated in argon matrices (27). However, the absence of an absorption near this frequency in the infrared spectra of 7MG and DMG coupled to the presence of a strong band at 1654 cm^{-1} in the spectrum of DMAG (where no absorption from the amino group is expected because of methylation) contradicts this assignment. Since this band is seen only in the infrared spectra of those compounds which have demonstrated the probability of existing in more than one tautomeric form in the matrix (9EG, DMAG, and G), we examined the possibility of this band arising from amino-hydroxy tautomers. Examination, in this frequency region, of the infrared spectrum of matrix-isolated isocytosine (26), which is known to exist mainly as its amino-hydroxy tautomer in the matrix, showed an absence of strong absorption near this

frequency. A band at 1655 cm^{-1} has been reported for cytosine isolated in an argon matrix (25,154), which exists as a mixture of its amino-oxo and amino-hydroxy tautomeric forms under these experimental conditions, and assigned to a C=C stretching mode. The absence of absorption in the spectra of 7MG and DMG led to the tentative assignment of this band to a combination of C=C double bond and C-N vibrations in the imidazole ring of the amino-hydroxy tautomers of G, 9EG, and DMAG. The lower frequency of this absorption band in 9EG (1644 cm^{-1}) as compared to 1654 cm^{-1} in G and DMAG could then be explained as a result of N(9)-methylation.

The infrared spectra of DMG and 7MG exhibit a strong absorption band at 1612 cm^{-1} and 1628 cm^{-1} , respectively. This band shows a splitting in G (1619 and 1628 cm^{-1}) and 9EG (1620 and 1624 cm^{-1}). No absorption was detected around this frequency with a similar intensity in the spectrum of matrix-isolated DMAG. The absence of this band in DMAG coupled to the prediction of two strong bands at 1634 and 1610 cm^{-1} for the amino-oxo monomer of G (152), led us to the assignment of these bands as arising from the amino group scissoring mode. The reason for the splitting of these bands in the infrared spectra of matrix-isolated G and 9EG is still unclear. A possible explanation is that it is due to the simultaneous presence of both the amino-hydroxy and amino-oxo tautomeric forms of these two compounds in the matrix.

A very complex structure is seen in the 1600-1580 cm^{-1} region of the infrared spectra of G, 9EG, and DMAG isolated in argon matrices (see Figure 20). The band splitting is seen in the spectra obtained from both (argon and nitrogen) matrices (thus ruling out matrix effects). No bands are predicted in this region, with such strong intensities, for the amino-oxo monomer of G (152). The absence of strong absorptions in the infrared spectra of the fixed oxo-form, DMG, as well as in those of 7MG, rules out the possibility of these bands arising from ring stretching vibrations of the amino-oxo tautomeric forms of G, 9EG, and DMAG. These bands are therefore tentatively assigned to ring stretching modes of the amino-hydroxy tautomers of these compounds.

For the final assignment of the absorption bands in the 1580-700 cm^{-1} we have used the following procedure:

1. The comparison of the spectra of guanine to those of its derivatives has proven to be most useful in making the assignments. It allowed us to identify the regions where methyl groups, as well as O-H, C-O, and some other vibrational modes appeared.
2. We have tried to assign first the strongest bands to the fundamental vibrations as predicted by ab initio calculations on guanine (152,153), and/or methyl groups.

3. The medium and weaker bands close to strong fundamentals were often assigned to arise from Fermi resonance of the strong bands with lower combination bands, unless weak or medium intensity fundamentals were expected in that region.
4. Splitting of some bands into two or more components were attributed in some cases to matrix effects.
5. Weak bands in regions in which we did not expect any fundamentals were assigned to combination bands.
6. Some weak bands could also arise from the presence in the matrix of non-identified impurities even though a high sublimation process was performed during the preparation of the matrix samples.
7. Out of plane modes were assigned on the basis of preliminary ab initio calculations for guanine (152,152).

In spite of all of these, the proposed assignment is very uncertain. It may change drastically when more experimental data for other guanine derivatives are available. It may also change when calculations for the different tautomeric forms of these molecules are performed.

Two strong bands are predicted by ab initio calculations for the amino-oxo tautomer of G at 1570 and 1523 cm^{-1} (152,153). Both were assigned to ring stretching modes. A strong absorption band with complex structure and subband at 1570, 1560, and 1554 cm^{-1} , and a medium intensity band at 1518 cm^{-1} were seen in the infrared spectrum of matrix-isolated DMG (see Figure 20). These ring stretching vibrations are expected to be coupled with methyl group bending modes. Weaker bands are seen at 1570 and 1550 cm^{-1} in DMAG, while three bands (1562, 1536, and 1521 cm^{-1}) were observed in the spectrum of 9EG isolated in an argon matrix. The spectrum of matrix-isolated G also exhibits three absorption bands at 1570, 1547, and 1534 cm^{-1} . They have been assigned to ring stretching vibrational modes. The infrared spectrum of DMG exhibits medium intensity bands at 1426, 1395, and 1355 cm^{-1} and a strong band at 1414 cm^{-1} . About the same intensity pattern is observed in 7MG with bands at 1427, 1413, 1380, and 1355 cm^{-1} . The 1335 cm^{-1} band is assigned to a combination of ring stretch and NH_2 bending modes and the others to ring vibrations with large contributions from methyl bending modes.

The weak absorption bands in the 1500-1300 and 1200-1100 cm^{-1} regions in the spectrum of DMAG have been assigned to ring stretching modes coupled to O-H bending vibrations. The infrared spectra of matrix-isolated 9EG and G exhibit a much more complex pattern with a number of medium and weak

intensity absorption bands in these regions. These were generally assigned to coupled vibrations of O-H and methyl (for 9EG) bending modes with ring stretching vibrations. The medium intensity bands observed in the $1300\text{--}1150\text{ cm}^{-1}$ region in the spectra of DMG and 7MG exhibited a strong contribution from methyl group absorption. The band at 1216 cm^{-1} in DMG and 1220 in 7MG are tentatively assigned to bending modes of methyl groups attached to the imidazole ring. A similar band is seen at about the same frequency in the spectrum of 9EG and attributed to the same vibrational mode. The band around 1190 cm^{-1} is observed only in the spectrum of DMG. It has been tentatively assigned to a bending mode of the methyl group attached to the N(1)-atom. A similar frequency was reported for the same vibrational mode in the infrared spectra of methylated uracils (20). The absence of appreciable absorption in this region in the infrared spectrum of G was taken as further proof for the contribution of methyl group absorption in this frequency region.

The spectrum of the fixed oxo-tautomeric form, DMG, as well as that of 7MG, showed a medium intensity band around 780 cm^{-1} . Ab initio calculations predicts a pyrimidine ring bending mode (out of plane) to appear at 796 cm^{-1} (152,153). Strikingly, two bands appeared in the infrared spectra of G, 9EG, and DMAG; one around 780 cm^{-1} and another at 790 cm^{-1} . Since the higher frequency band is only seen in the infrared spectra of those compounds which exhibited the possibility of

existing in the matrix in more than one tautomeric form; we have tentatively assigned these bands in G, 9EG, and DMAG to ring bending modes of their amino-hydroxy forms.

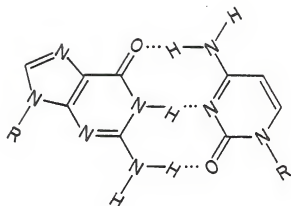
CHAPTER V

CONCLUSIONS AND RECOMMENDATIONS

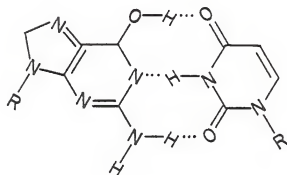
The results presented here strongly suggest that monomeric molecules of guanine (G), 9-ethylguanine (9EG), and 2-N,N-dimethylaminoguanine (DMAG) are present in the matrix in more than one tautomeric form when isolated in inert matrices (argon and nitrogen). Absorption bands arising from O-H ($3580\text{--}3560\text{ cm}^{-1}$) and C=O ($1750\text{--}1730\text{ cm}^{-1}$) stretching modes were identified in their infrared spectra and taken as proof of the simultaneous presence of the oxo and hydroxy tautomers of these compounds in the matrices. The presence of absorption bands attributed to vibrational modes of the amino group ($3550\text{--}3520\text{ cm}^{-1}$ for the asymmetric stretch, $3440\text{--}3420\text{ cm}^{-1}$ for the symmetric stretch, and $1640\text{--}1610\text{ cm}^{-1}$ for the scissoring mode) identified the amino tautomeric forms of guanine (G), 7-methylguanine (7MG), 9-ethylguanine (9EG), and 1,7-dimethylguanine (DMG). In addition the splitting of the bands in the $3500\text{--}3480\text{ cm}^{-1}$ frequency region was attributed to the simultaneous presence of the N(9)-H and N(7)-H tautomers of guanine (G) and 2-N,N-dimethylaminoguanine (DMAG) in the matrices.

The observation that isolated molecules of guanine (G), 9-ethylguanine (9EG), and 2-N,N-dimethylaminoguanine (DMAG) exists in both their oxo and hydroxy forms cannot be extended directly to these molecules when they occur in nucleic acids. However, this property is a physico-chemical characteristic of these compounds and it can manifest itself in one of the numerous stages of nucleic acid metabolism in a living cell. It is evident, then, that during transitions to its hydroxy form, the complementary pair for guanine (G) will be thymine (T) or uracil (U) rather than cytosine (C) (see Figure 21). It is interesting to note, in this connection, that experimental errors in codon-anticodon recognition include only situations in which guanine (G) has been incorrectly bonded to uracil (157). Furthermore, only the members of the G-C complementary pair have been shown to exist in more than one tautomeric form in inert matrices (24,29,154, and this work).

The effect of substituents on the oxo-hydroxy tautomeric equilibria is clearly established from the comparison of the tautomeric forms observed in the infrared spectra of 7-methylguanine (7MG) isolated in inert matrices to those exhibited by 9-ethylguanine (9EG). While only the amino-oxo tautomeric form was detected for 7-methylguanine (7MG), both the amino-oxo and amino-hydroxy forms were seen in the infrared spectra of 9-ethylguanine (9EG) isolated in inert matrices (see Table VIII). These experimental results have



"Correct" G-C Pair



"Incorrect" G*-U Pair

Figure 21. "Correct" G-C Pair and
"Incorrect" G*-U Pair.

TABLE VIII
Tautomeric Forms of Guanine and Its Derivatives in Argon
and Nitrogen Matrices and in the Solid State

Compound	Tautomeric Forms in an Argon Matrix	Tautomeric Forms in a Nitrogen Matrix	Tautomeric Forms in the Solid State
G	amino-oxo amino-hydroxy	amino-oxo amino-hydroxy	amino-oxo
9EG	amino-oxo amino-hydroxy	amino-oxo amino-hydroxy	amino-oxo
DMAG	amino-oxo amino-hydroxy	amino-oxo amino-hydroxy	amino-oxo
7MG	amino-oxo	amino-oxo	amino-oxo
DMG	amino-oxo	amino-oxo	amino-oxo

been interpreted in this work as proof of the importance of the N(7)-position in stabilizing hydroxy forms through intramolecular hydrogen-bonding (as depicted in form 4 for 9-ethylguanine in Figure 17).

The spectrum of associated species in the disordered solid state (solids deposited at 10 K and no annealing) differ significantly from the spectra obtained from the crystalline (KBr) solids. The most dramatic changes are observed in the N-H stretching ($3600-1800\text{ cm}^{-1}$) and in-plane N-H bending and C=O stretching ($1700-1500\text{ cm}^{-1}$) regions. This may implied that the strength of the interaction and probably the type of hydrogen-bonding may be different in the associated species in the disordered solid that in the crystalline (KBr) solid. Similar results have been reported for 1-methyluracil (21). It is clear that the matrix-isolation technique is of considerable utility for the examining the vibrational spectra of monomeric (or matrix-isolated) nucleic acid bases. The vibrational spectra obtained from matrix-isolated samples are very similar to those obtained from studies performed in the vapor phase (14,16). This observation supports other studies (14,15,17-29,154-156) and should be of practical use inasmuch as the matrix-isolation method may be applied to studies of compounds that are unstable at the higher temperatures required for vapor phase studies.

The present results were found to be consistent with those obtained from theoretical calculations on the amino-oxo monomer of guanine (152,153). Of course, consistency means the same assignment for the principal bands, and it is natural that some discrepancies may occur since theoretical calculations are not accurate either. Even the best calculations on guanine at the ab initio level (152), differ from the experimental data and only a careful and systematic scaling leads to a better reproduction of the experimental spectrum. The presence of more than one tautomeric form in the matrices coupled to the lack of reliable theoretical calculations for other tautomeric forms as well as for guanine derivatives makes the proposed assigned uncertain. It may change drastically when more experimental data for other guanine derivatives (especially a fixed amino-hydroxy derivative) as well as for isotopically substituted (with D,O18, N15) molecules are available.

APPENDIX A

INFRARED SURVEY SPECTRA IN THE 3900-700 cm^{-1} REGION

<u>Figure</u>		<u>Page</u>
A.1	Infrared Survey Spectrum of 1,7-dimethyl- guanine Isolated in an Argon Matrix	102
A.2	Infrared Survey Spectrum of 1,7-dimethyl- guanine Isolated in a Nitrogen Matrix	103
A.3	Infrared Survey Spectrum of a Polycrystalline Film of 1,7-dimethylguanine Deposited at 10 K (no Annealing)	104
A.4	Infrared Survey Spectrum of 1,7-dimethyl- guanine in the Solid State (KBr Pellets)	105
A.5	Infrared Survey Spectrum of 7-methylguanine Isolated in an Argon Matrix	106
A.6	Infrared Survey Spectrum of 7-methylguanine Isolated in a Nitrogen Matrix	107
A.7	Infrared Survey Spectrum of a Polycrystalline Film of 7-methylguanine Deposited at 10 K (no Annealing)	108
A.8	Infrared Survey Spectrum of 7-methylguanine in the Solid State (KBr Pellets)	109
A.9	Infrared Survey Spectrum of 2-N,N-dimethyl- aminoguanine Isolated in an Argon Matrix	110
A.10	Infrared Survey Spectrum of 2-N,N-dimethyl- aminoguanine Isolated in a Nitrogen Matrix ...	111
A.11	Infrared Survey Spectrum of a Polycrystalline Film of 2-N,N-dimethylaminoguanine Deposited at 10 K (no Annealing)	112

A.12	Infrared Survey Spectrum of 2-N,N-dimethyl-aminoguanine in the Solid State (KBr Pellets)	113
A.13	Infrared Survey Spectrum of 9-ethylguanine Isolated in an Argon Matrix	114
A.14	Infrared Survey Spectrum of 9-ethylguanine Isolated in a Nitrogen Matrix	115
A.15	Infrared Survey Spectrum of a Polycrystalline Film of 9-ethylguanine Deposited at 10 K (no Annealing)	116
A.16	Infrared Survey Spectrum of 9-ethylguanine in the Solid State (KBr Pellets)	117
A.17	Infrared Survey Spectrum of Guanine Isolated in an Argon Matrix	118
A.18	Infrared Survey Spectrum of Guanine Isolated in a Nitrogen Matrix	119
A.19	Infrared Survey Spectrum of a Polycrystalline Film of Guanine Deposited at 10 K (no Annealing)	120
A.20	Infrared Survey Spectrum of Guanine in the Solid State (KBr Pellets)	121

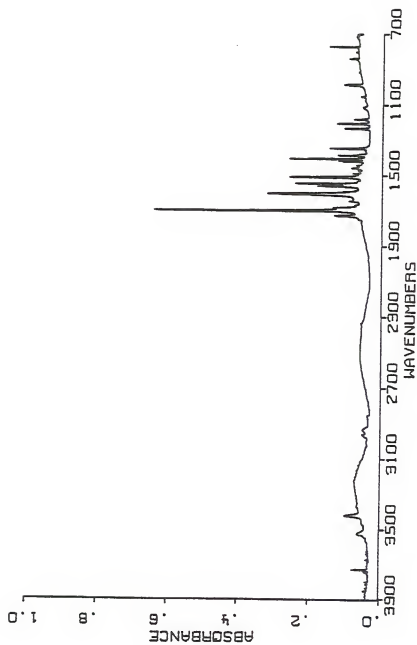


Figure A.1. Infrared Spectrum of 1,7-dimethylguanine Isolated in an Argon Matrix.

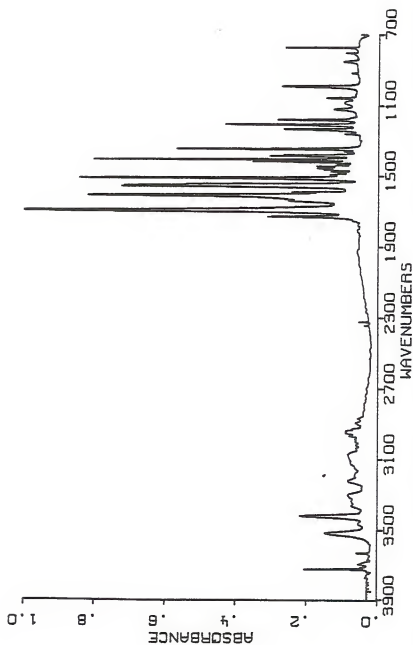


Figure A.2. Infrared Spectrum of 1,7-dimethylguanidine Isolated in a Nitrogen Matrix.

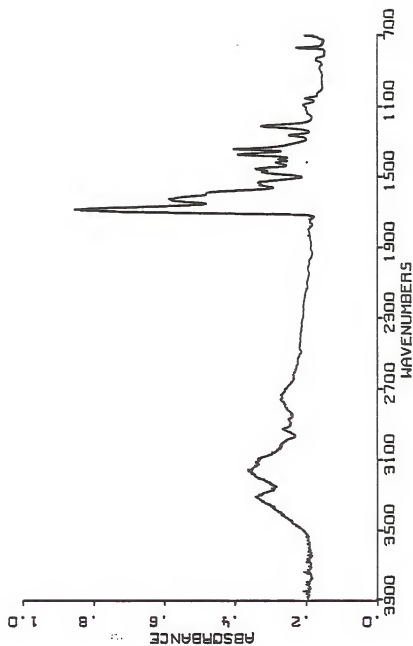


Figure A.3. Infrared Spectrum of a Polycrystalline Film of 1,7-dimethylguanine Deposited at 10°K (no Annealing).

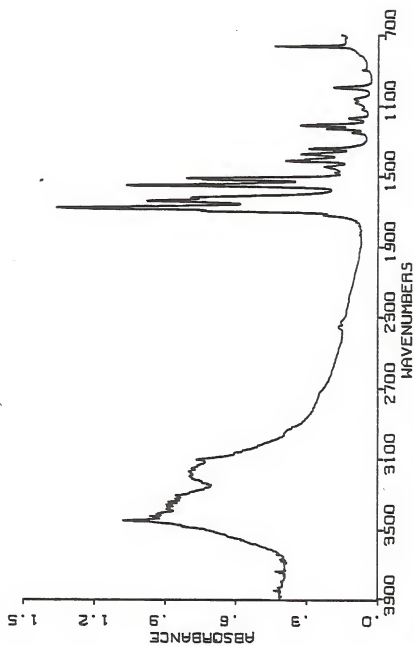


Figure A.4. Infrared Spectrum of 1,7-dimethylguanidine in the Solid State (KBr Pellet).

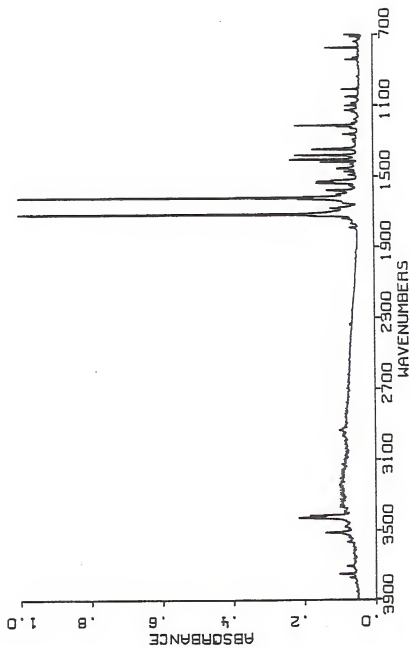


Figure A.5. Infrared Spectrum of 7-methylguanine Isolated in an Argon Matrix.

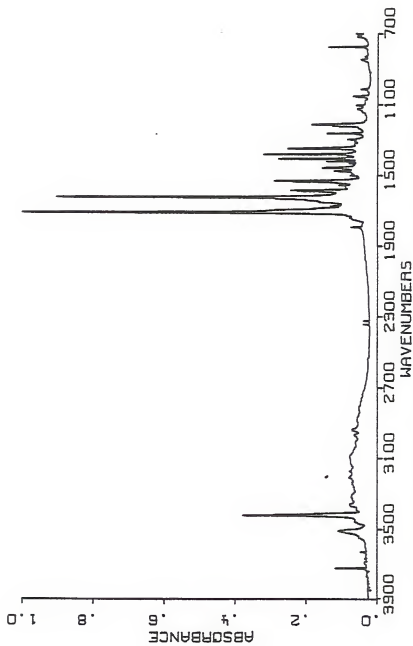


Figure A.6. Infrared Spectrum of 7-methylguanine Isolated in a Nitrogen Matrix.

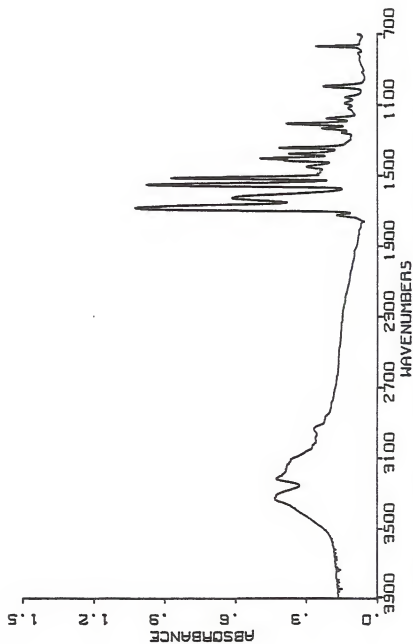


Figure A.7. Infrared Spectrum of a Polycrystalline Film of 7-methylguanine Deposited at 10°K (no Annealing).

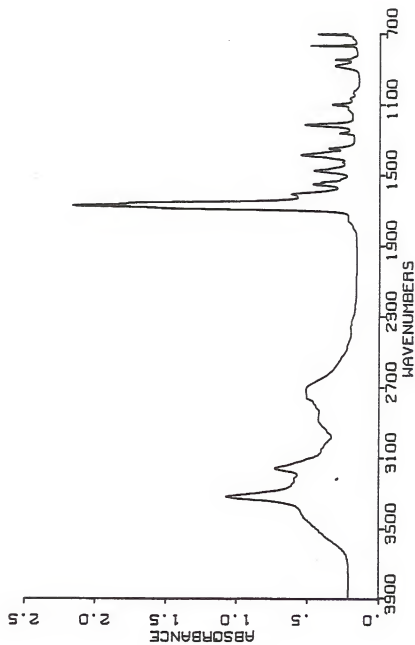


Figure A.8. Infrared Spectrum of 7-methylguanine in the Solid State (KBr Pellets).

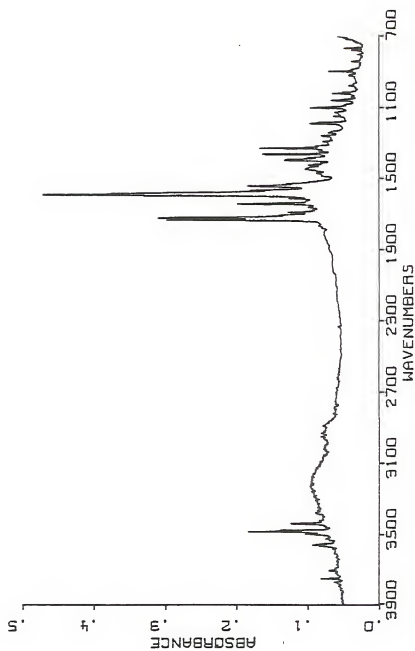


Figure A.9. Infrared Spectrum of 2-N,N-dimethylaminoguanine Isolated in an Argon Matrix.

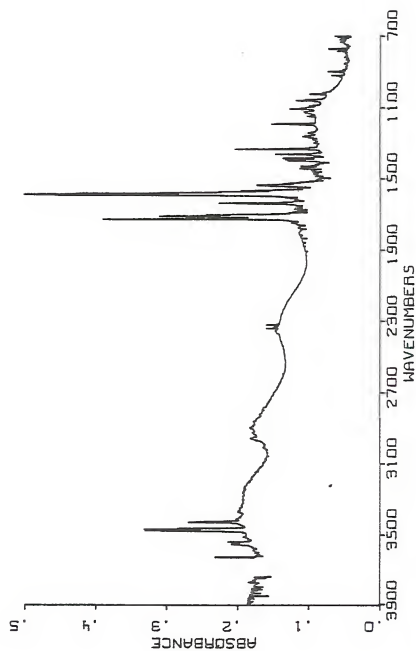


Figure A.10. Infrared Spectrum of 2-N,N-dimethylaminoguanine Isolated in a Nitrogen Matrix.

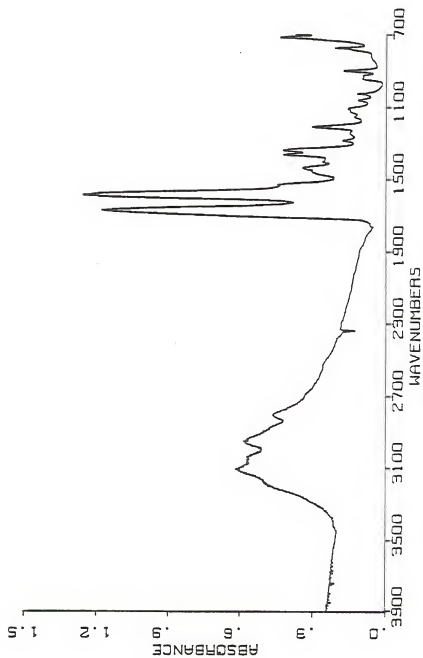


Figure A.11. Infrared Spectrum of a Polycrystalline Film of 2-N,N-dimethylaminoguanine Deposited at 10°K (no Annealing).

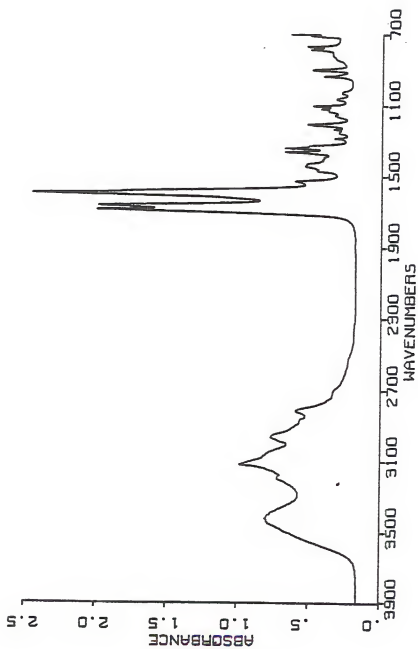


Figure A.12. Infrared Spectrum of 2-N,N-dimethylaminoguanine in the Solid State (KBr Pellets).

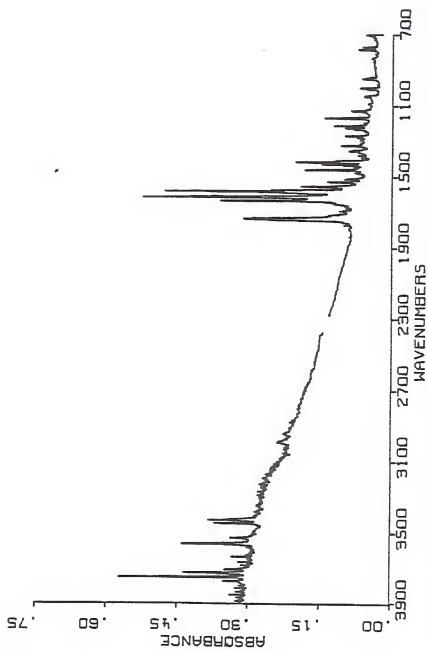


Figure A.13. Infrared Spectrum of 9-ethylguanine Isolated in an Argon Matrix.

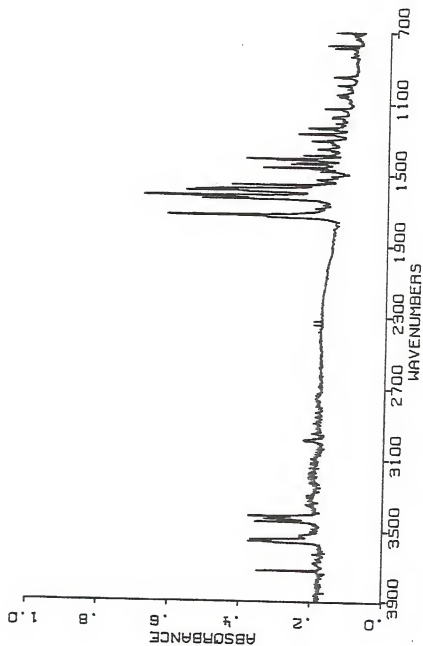


Figure A.14. Infrared Spectrum of 9-ethylguanine Isolated in a Nitrogen Matrix.

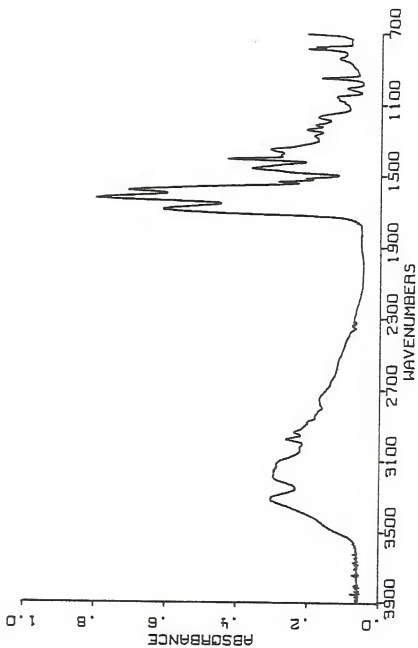


Figure A.15. Infrared Spectrum of a Polycrystalline Film of 9-thyiguanine Deposited at 10°K (no Annealing).

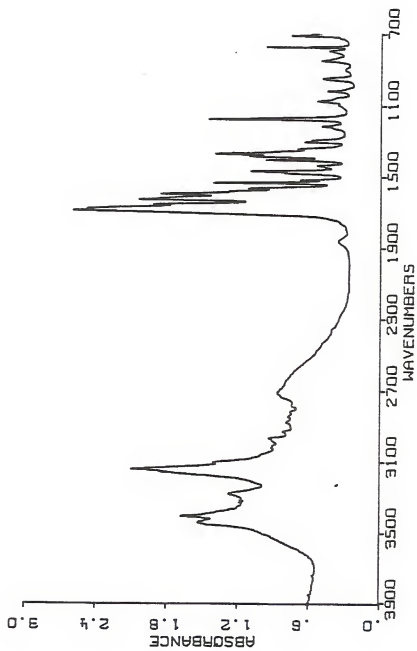


Figure A.16. Infrared Spectrum of 9-ethylguanine in the Solid State (KBr Pellets).

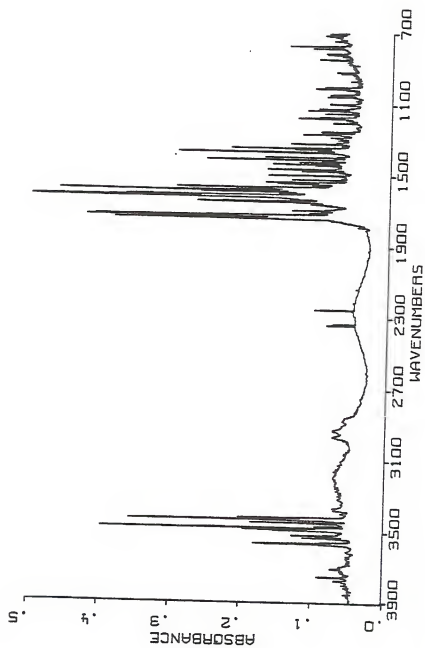


Figure A.17. Infrared Spectrum of Guanine Isolated in an Argon Matrix.

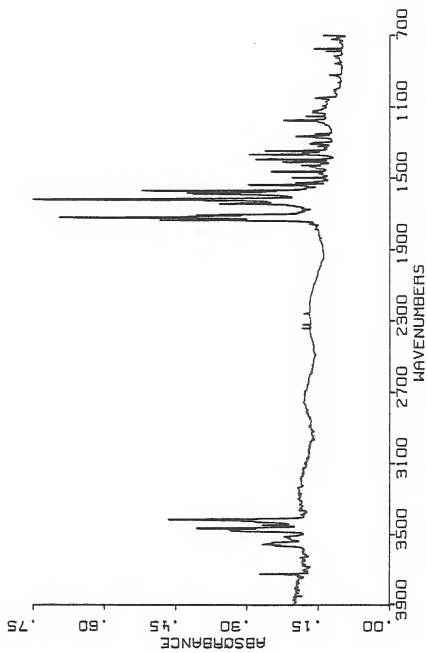


Figure A.18. Infrared Spectrum of Guanine Isolated in a Nitrogen Matrix.

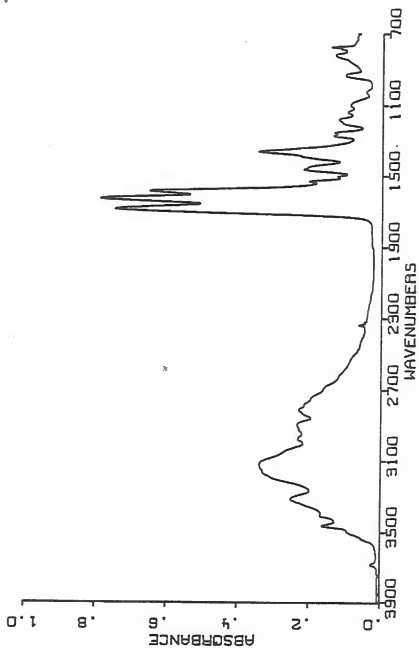


Figure A.19. Infrared Spectrum of Polycrystalline Film of Guanine Deposited at 10°K (no Annealing).

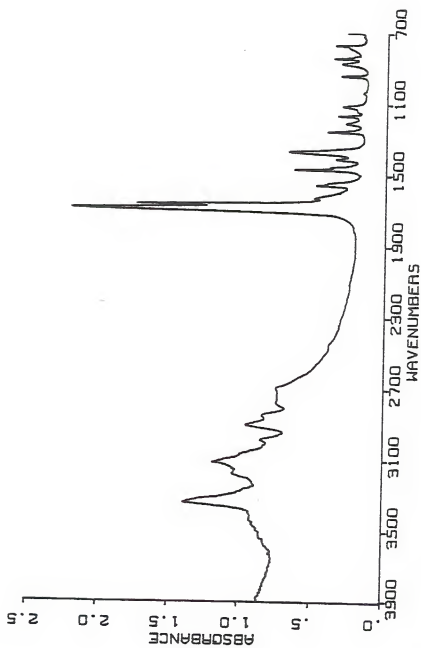


Figure A.20. Infrared Spectrum of Guanine in the Solid State (KBr Pellets).

APPENDIX B

INFRARED SPECTRA OF ISOLATED MOLECULES IN ARGON AND NITROGEN MATRICES IN THE 3600-3400 cm^{-1} REGION

LIST OF FIGURES

<u>Figure</u>		<u>Page</u>
B.1	Infrared Spectra of 1,7-dimethylguanine Isolated in Argon and Nitrogen Matrices	123
B.2	Infrared Spectra of 7-methylguanine Isolated in Argon and Nitrogen Matrices	124
B.3	Infrared Spectra of 2-N,N-dimethylamino- guanine Isolated in Argon and Nitrogen Matrices	125
B.4	Infrared Spectra of 9-ethylguanine Isolated in Argon and Nitrogen Matrices	126
B.5	Infrared Spectra of Guanine Isolated in Argon and Nitrogen Matrices	127

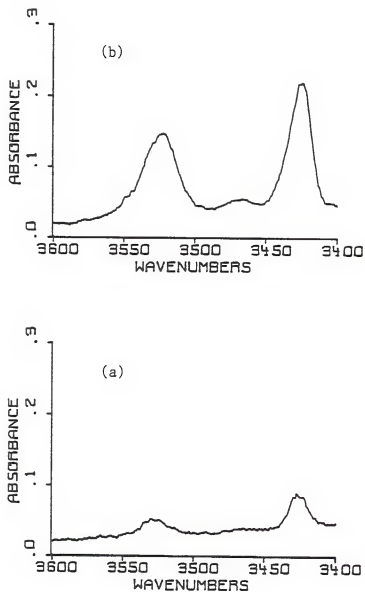


Figure B.1. Infrared Spectra of 1,7-dimethylguanine Isolated in:
(a) Argon and (b) Nitrogen Matrices.

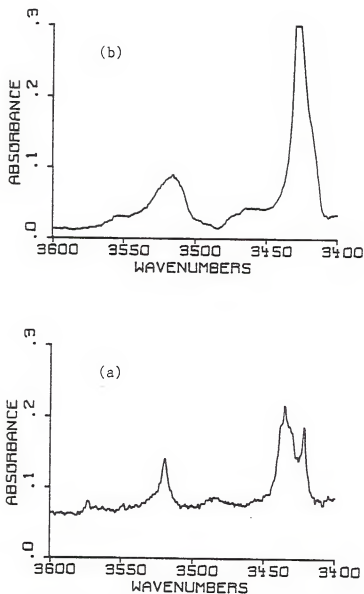


Figure B.2. Infrared Spectra of 7-methylguanine Isolated in:
(a) Argon and (b) Nitrogen Matrices.

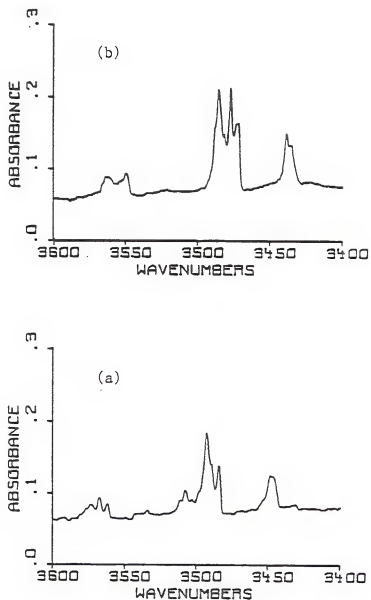


Figure B.3. Infrared Spectra of 2-N,N-dimethylaminoguanine Isolated in: (a) Argon and (b) Nitrogen Matrices.

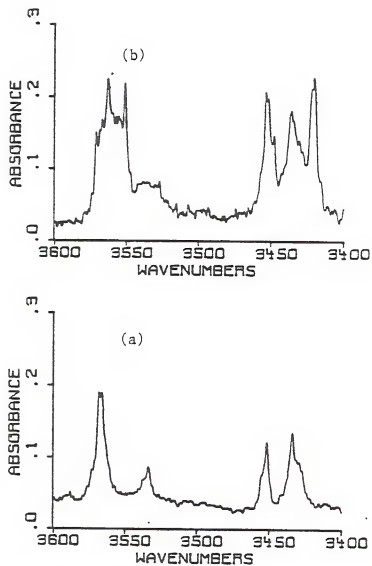


Figure B.4. Infrared Spectra of 9-ethylguanine Isolated in:
(a) Argon and (b) Nitrogen Matrices.

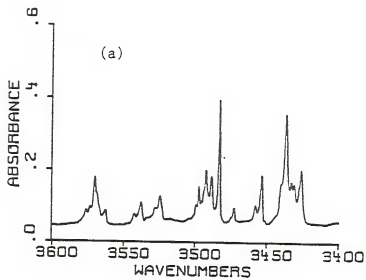
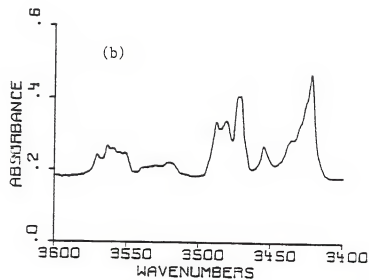


Figure B.5. Infrared Spectra of Guanine Isolated in: (a) Argon and (b) Nitrogen Matrices.

APPENDIX C
INFRARED SPECTRA OF ISOLATED MOLECULES
IN ARGON AND NITROGEN MATRICES IN THE 1800-700 cm^{-1} REGION

LIST OF FIGURES

<u>Figure</u>	<u>Page</u>
C.1 Infrared Spectra of 1,7-dimethylguanine Isolated in Argon and Nitrogen Matrices	129
C.2 Infrared Spectra of 7-methylguanine Isolated in Argon and Nitrogen Matrices	134
C.3 Infrared Spectra of 2-N,N-dimethylamino- guanine Isolated in Argon and Nitrogen Matrices	139
C.4 Infrared Spectra of 9-ethylguanine Isolated in Argon and Nitrogen Matrices	144
C.5 Infrared Spectra of Guanine Isolated in Argon and Nitrogen Matrices	149

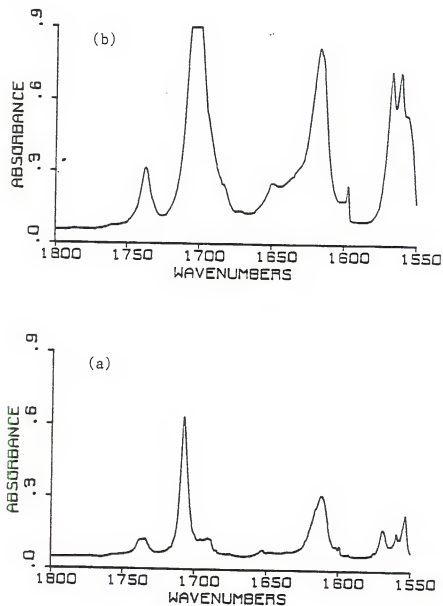


Figure C.1. Infrared Spectra of 1,7-dimethylguanine Isolated in:
(a) Argon and (b) Nitrogen Matrices.

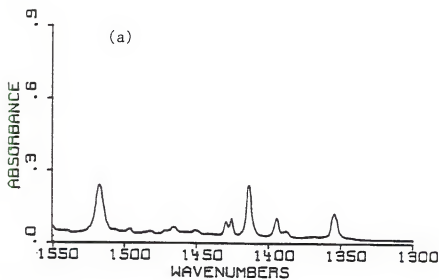
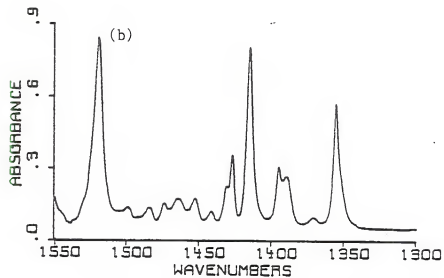


Figure C.1.--continued

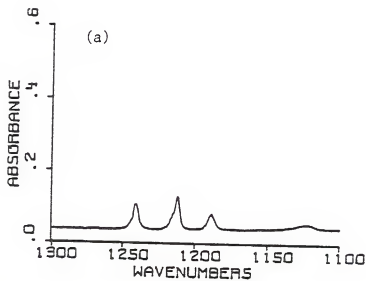
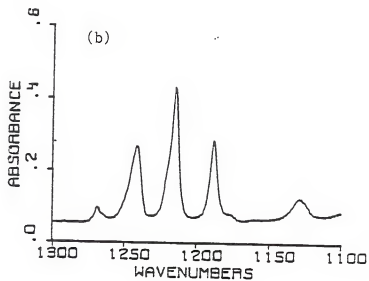


Figure C.1.--continued

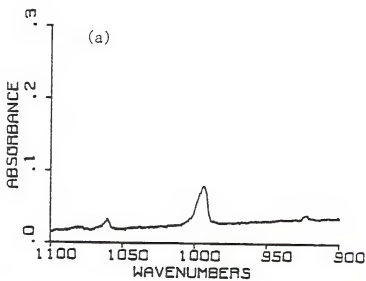
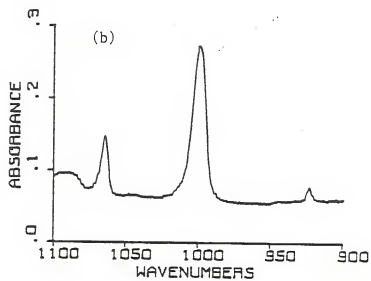


Figure C.1.--continued

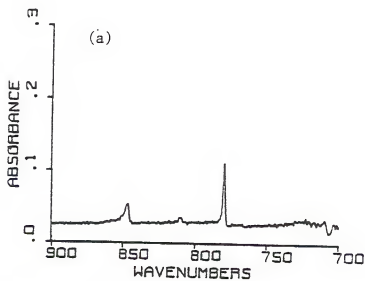
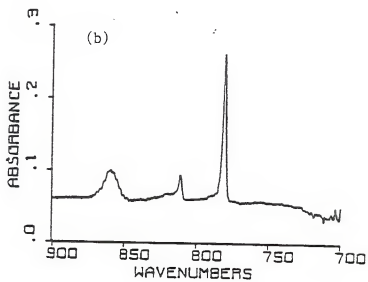


Figure C.1.--continued

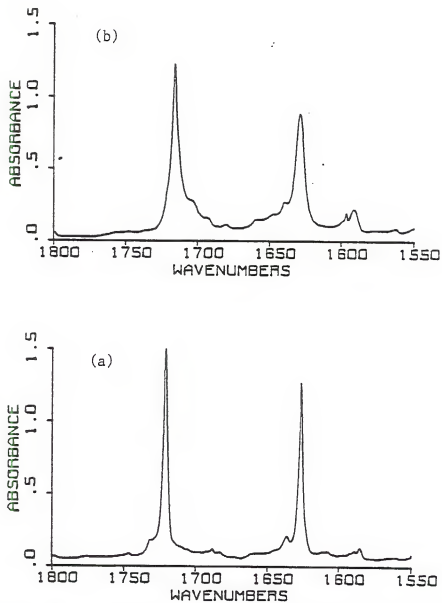


Figure C.2. Infrared Spectra of 7-methylguanine Isolated in: (a) Argon and (b) Nitrogen Matrices.

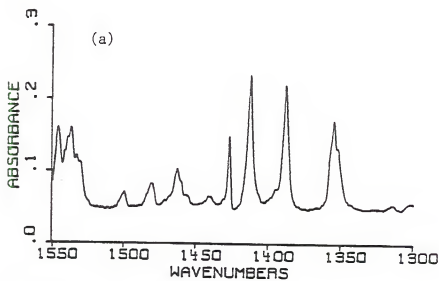
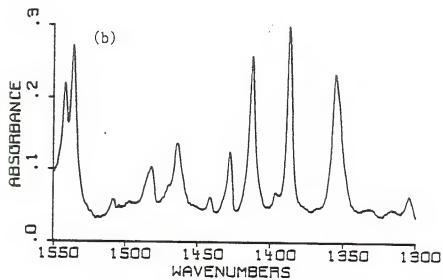


Figure C.2.--continued

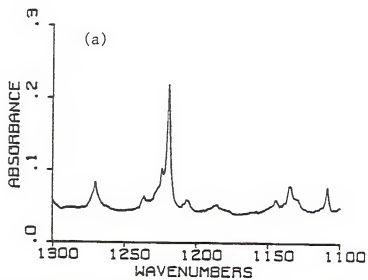
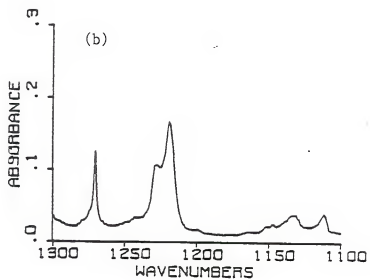


Figure C.2.--continued

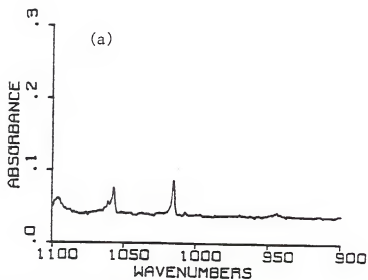
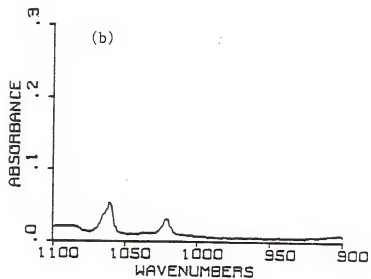


Figure C.2.--continued

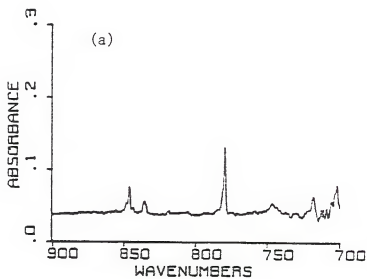
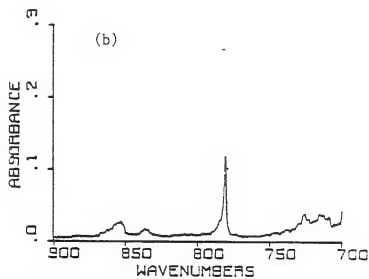


Figure C.2.--continued

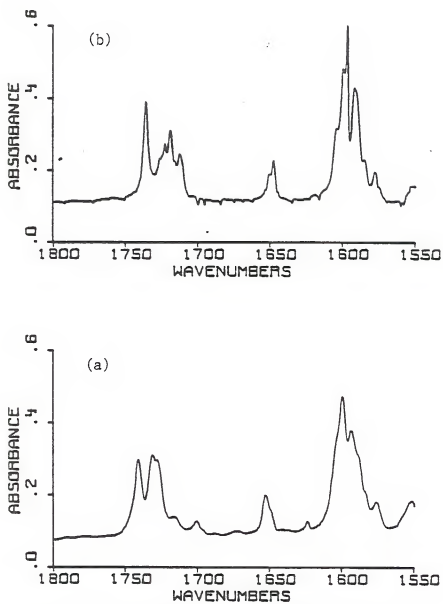


Figure C.3. Infrared Spectra of 2-N,N-dimethylaminoguanine
Isolated in: (a) Argon and (b) Nitrogen Matrices.

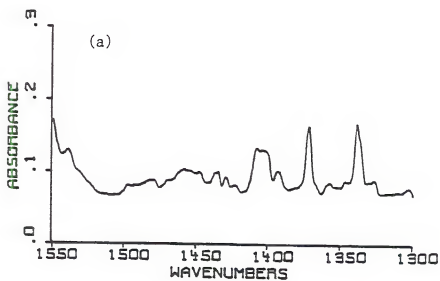
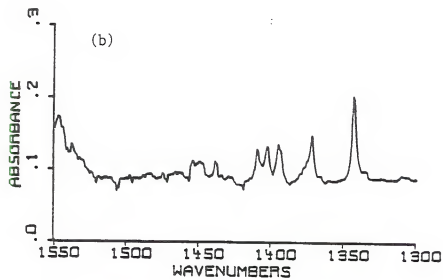


Figure C.3.--continued

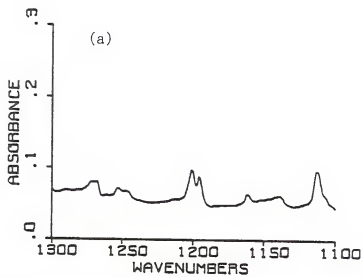
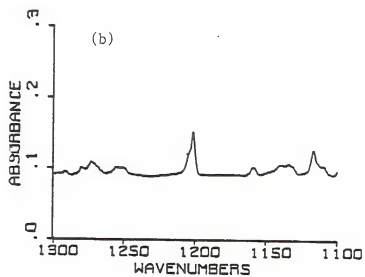


Figure C.3.--continued

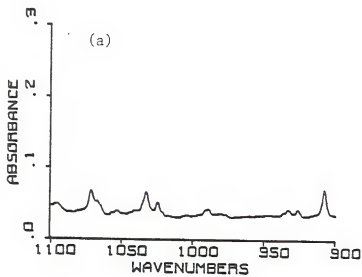
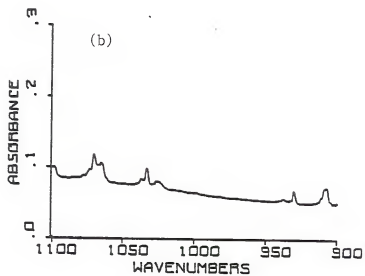


Figure C.3.--continued

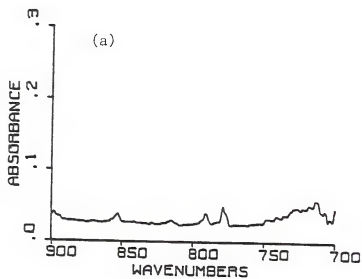
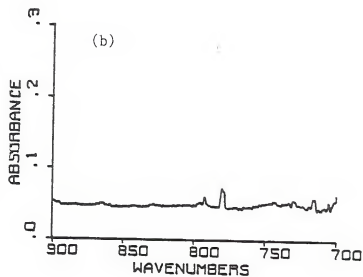


Figure C.3.--continued

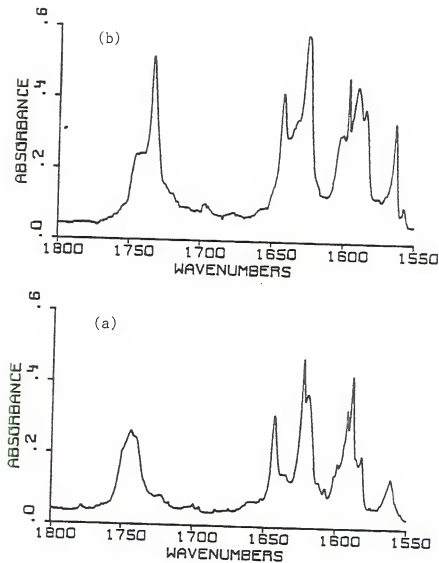


Figure C.4. Infrared Spectra of 9-ethylguanine Isolated in:
(a) Argon and (b) Nitrogen Matrices.

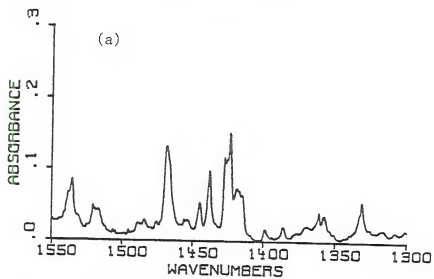
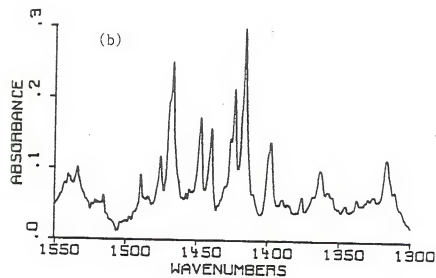


Figure C.4.--continued

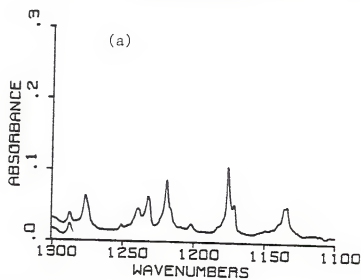
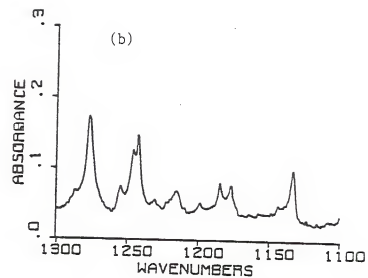


Figure C.4.--continued

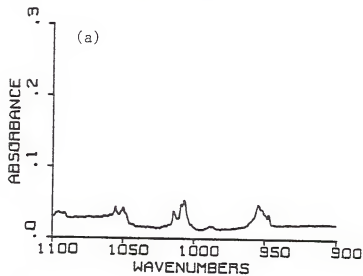
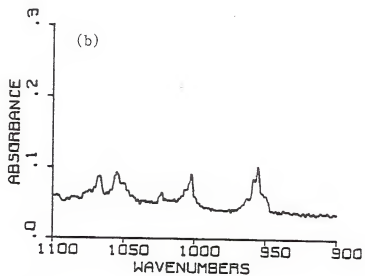


Figure C.4.--continued

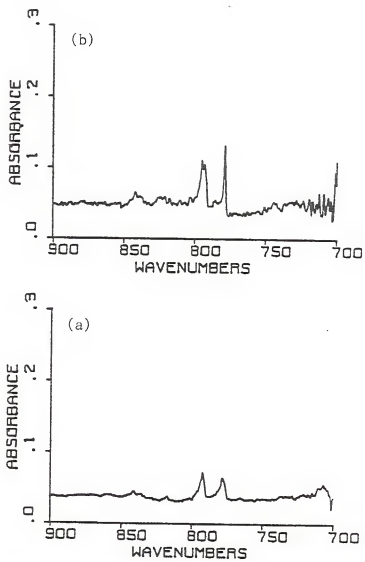


Figure C.4.--continued

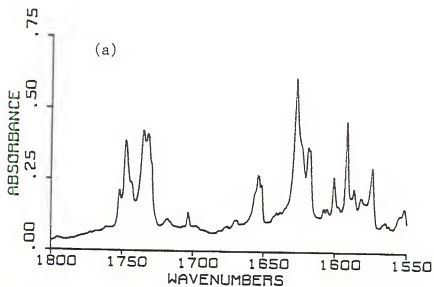
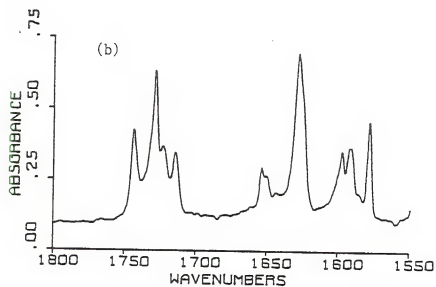


Figure C.5. Infrared Spectra of Guanine Isolated in: (a) Argon and (b) Nitrogen Matrices.

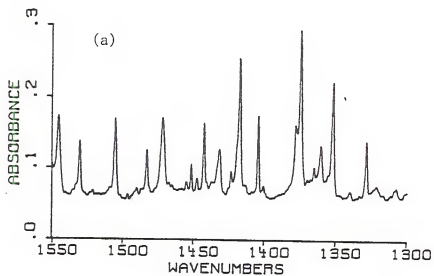
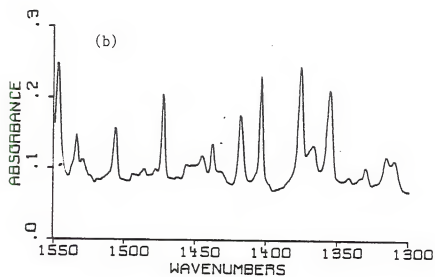


Figure C.5.--continued

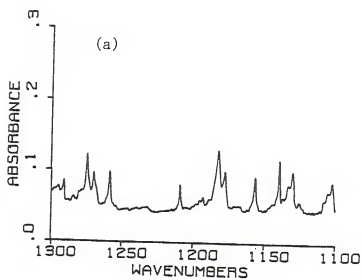
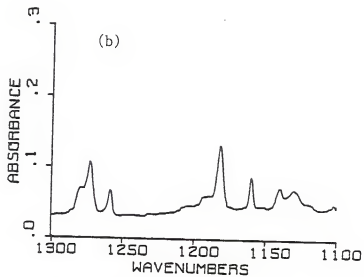


Figure C.5.--continued

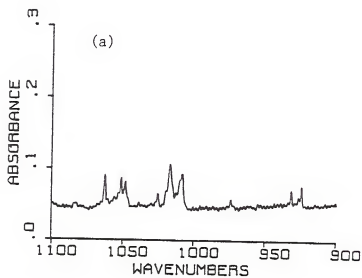
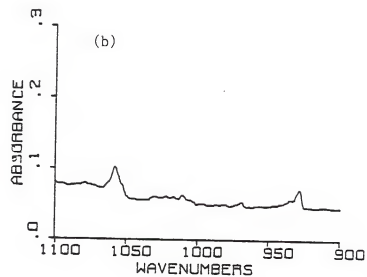


Figure C.5.--continued

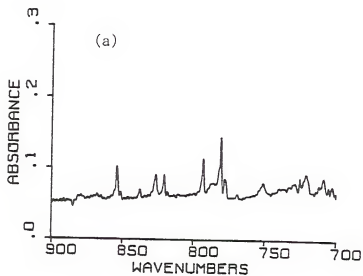
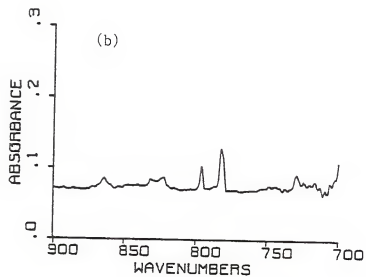


Figure C.5.--continued

REFERENCES

1. Katritzky, A. R., and Lagowski, J. M., Adv. Heterocycl. Chem., 1963, 1, 311.
2. Katritzky, A. R., and Ambler, P. A., in "Physical Methods in Heterocyclic Chemistry" (Academic Press, New York) 1963, 2, p. 161.
3. Elguero, J., Marzin, C., Katritzky, A. R., and Linda, P., Adv. Heterocycl. Chem., 1975, Suppl. 1.
4. Kwiatkowski, J. S., Zielinski, T. J., and Rein, R., Adv. Quantum Chem. 1986, 18, 85.
5. Lowdin, P. O., Adv. Quantum Chem., 1965, 2, 213.
6. Cooper, W. G., Int. J. Quantum Chem., 1978, 14, 71.
7. Rein, R., Shibata, M., Garduno-Juarez, R., and Kieber--Emmons, T., in "Structure and Dynamics: Nucleic Acids and Proteins" (Adenine, New York) 1983, p. 269.
8. Metzler, J. D., Adv. Enzymology, 1979, 50, 1.
9. Hall, R. H., in "The Modified Nucleosides in Nucleic Acids and Proteins" (Columbia University Press, New York and London) 1971. p. 17.
10. Bendich A., in "The Nucleic Acids" (Academic Press, New York), 1955, 1, p.81.
11. Mahler, H. A., and Cordes, E. H., in "Basic Biological Chemistry" (Harper & Row Publishers, New York, Evanston, and London) 1968.
12. Bloch, A., Ann. N. Y. Acad. Sci., 1975, 255, 576.
13. Shugar, D., and Kierdaszuk, B., Proc. Int. Symp. Biomol. Struct. Interactions (Biosci.), 1985, Suppl. J (8), 657.

14. Nowak, M. J., Szczepaniak, K., Barski, A., and Shugar, D., *J. Mol. Struct.*, 1980, 62, 47.
15. Shugar, D., and Szczepaniak, K., *Int. J. Quantum Chem.*, 1981, 20, 573.
16. Nowak, M. J., Szczepaniak, K., Barski, A., and Shugar, D., *Z. Naturforsch.* 1978, 33C, 876.
17. Szczesniak, M., Nowak, M. J., Rostkowska, H., Szczepaniak, K., Person, W. B., and Shugar, D., *J. Am. Chem. Soc.*, 1983, 105, 5969.
18. Chin, S., Scott, I., Szczepaniak, K., and Person, W. B., *J. Am. Chem. Soc.*, 1984, 106, 3415.
19. Szczepaniak, K., Szczesniak, M., Nowak, M. J., Scott, I., Chin, S., and Person, W. B., *Int. J. Quantum Chem.*, 1984, 18, 547.
20. Szczesniak, M., Nowak, M. J., Szczepaniak, K., Chin, S., Scott, I., and Person, W. B., *Spectrochim. Acta*, 1985, 41A, 223.
21. Szczesniak, M., Nowak, M. J., Szczepaniak, K., and Person, W. B., *Spectrochim. Acta*, 1985, 41A, 237.
22. Barnes, A. J., Stuckey, M. A., and LeGall, L., *Spectrochim. Acta*, 1984, 40A, 419.
23. Maltese, M., Passerini, S., Nunziante-Cesaro, S., Dobos, S., and Harsanyi, L., *J. Mol. Struct.*, 1984, 116, 49.
24. Radchenko, Y. D., Sheina, G. G., Smorygo, N. A., and Blagoi, Y. P., *J. Mol. Struct.*, 1984, 116, 387.
25. Radchenko, Y. D., Plokhonichenko, A. M., Sheina, G. G., and Blagoi, Y. P., *Biophysics*, 1983, 28, 592.
26. Szczesniak, M., Nowak, M. J., and Szczepaniak, K., *J. Mol. Struct.*, 1984, 115, 221.
27. Radchenko, Y. D., Plokhonichenko, A. M., Sheina, G. G., and Blagoi, Y. P., *Biophysics*, 1984, 29, 602.
28. Szczepaniak, K., and Szczesniak, M., *J. Mol. Struct.*, 1987, 156, 29.
29. Sheina, G. G., Radchenko, Y. D., Stepanian, S. G., and Blagoi, Y. P., *Stud. Biophys.*, 1986, 114, 223.

30. Czerminsky, R., Kuzcera, K., Rostkowska, H., Nowak, M. J., and Szczepaniak, K., *J. Mol. Struct.*, 1980, 140, 235.
31. Saenger, W., in "Principles of Nucleic Acid Structure" (Springer-Verlag, New York, Berlin, Heidelberg, Tokyo) 1984, p. 9.
32. Watson, J. D., and Crick, F. H. C., *Nature*, 1953, 171, 737.
33. Watson, J. D., and Crick, F. H. C., *Proc. Roy. Soc. (London)*, 1954, 223A, 80.
34. Saenger, W., in "Principles of Nucleic Acid Structure" (Springer-Verlag, New York, Berlin, Heidelberg, Tokyo) 1984, p. 116.
35. Parish, J. H., in "Principles and Practice of Experiments with Nucleic Acids" (Longman Group Limited, London) 1972.
36. Pullman, A., in "Electronic Aspects of Biochemistry" (Academic Press, New York) 1964, p. 135.
37. Psoda, A., and Shugar, D., *Biochim. Biophys. Acta*, 1971, 247, 507.
38. Gordon, A., and Katritzky, A. R., *Tetrahedron Lett.*, 1968, 2767.
39. Sepiol, J., Kazimierczuk, A. R., and Shugar, D., *Z. Naturforsch.*, 1970, 310, 361.
40. Cook, M. J., Katritzky, A. R., Linda, P., and Track, R. D., *J. Chem. Soc., Perkin Trans. 2*, 1972, 1295.
41. Levin, E. S., and Radionova, G. N., *Dokl. Akad. Nauk. SSSR*, 1967, 174, 1132.
42. Levin, E. S., and Radionova, G. N., *Dokl. Akad. Nauk. SSSR*, 1965, 164, 584.
43. Levin, E. S., and Radionova, G. N., *Dokl. Chem.*, 1969, 189, 900.
44. Beak, P., and Fry, F. S., *J. Am. Chem. Soc.*, 1973, 95, 1700.
45. Beak, P., Fry, F. S., Lee, J. L., and Steele, F., *J. Am. Chem. Soc.*, 1976, 98, 171.

46. Beak, P., Covington, J. B., and Smith, S. G., J. Am. Chem. Soc., 1976, 98, 3284.
47. Beak, P., and Covington, J. B., J. Am. Chem. Soc., 1978, 100, 3969.
48. Beak, P., and Covington, J. B., J. Org. Chem., 1978, 43, 177.
49. Beak, P., Acc. Chem. Res., 1977, 10, 186.
50. Parry, G. S., Acta Crystallogr., 1954, 7, 313.
51. Stewart, R. F., and Jensen, L. H., Acta Crystallogr., 1967, 23, 1102.
52. Osekil, K., Sakabe, N., and Tanaka, J., Acta Crystallogr., 1969, 25B, 1038.
53. Gerdil, R., Acta Crystallogr., 1961, 14, 333.
54. Green, D. W., Mathews, F. S., and Rich, A., J. Biol. Chem., 1962, 237, 3573.
55. Hoogsteen, K., Acta Crystallogr., 1963, 16, 28.
56. Reeke, G. N., and Marsh, R. E., Acta Crystallogr., 1966, 20, 703.
57. Craven, B. M., Acta Crystallogr., 1967, 23, 376.
58. Mizuno, H., Nakanishi, N., Fujiwara, T., Tomita, K., Tsukihara, T., Ashida, T., and Nakudo, M., Biochim. Biophys. Res. Commun., 1970, 41, 1161.
59. Shefter, E., J. Chem. Soc., Part B, 1970, 903.
60. Mizuno, H., Fujiwara, T., and Tomita, K., Bull. Chem. Soc. Jpn., 1972, 45, 909.
61. Destro, R., and Marsh, R. E., Acta Crystallogr., 1972, 28B, 2971.
62. Sundaralingam, M., J. Am. Chem. Soc., 1973, 95, 2333.
63. Singh, P., and Hodgson, D. J., J. Chem. Soc. Chem. Commun., 1973, 439.
64. Short, L. N., and Thompson, H. W., J. Chem. Soc., 1952, 168.
65. Angell, C. L., J. Chem. Soc., 1961, 504.

66. Miles, H. T., *Biochim. Biophys. Acta*, 1956, 22, 247.
67. Tanner, E. M., *Spectrochim. Acta*, 1956, 8, 9.
68. Miles, H. T., *Biochim. Biophys. Acta.*, 1958, 27, 46.
69. Frietzsche, H., and Hartmann, M., *Z. Chem.*, 1971, 11, 69.
70. Shimanouchi, T., Tsuboi, M., and Kyoguku, Y., *Adr., Chem. Phys.*, 1964, 7, 435.
71. Tinoco, I., and Halcomb, D. N., *Annu. Rev. Phys. Chem.*, 1964, 15, 371.
72. Nakanishi, K., Suzuki, N., and Yamasaki, P., *Bull. Chem. Soc. Jpn.*, 1961, 34, 53.
73. Susi, H., and Ard, J. S., *Spectrochim. Acta*. 1974, 30A, 1843.
74. Lewis, T. P., Miles, H. T., and Becker, E. D., *J. Phys. Chem.*, 1984, 88, 3253.
75. Lord, R. C., and Thomas, G. H., *Spectrochim. Acta*, 1974, 30A, 1843.
76. Lord, R. C., and Thomas, G. H., *Develop. Appl. Spectrosc.*, 1968, 6, 179.
77. Kokko, J. P., Goldstein, J. H., and Mandell, L., *J. Am. Chem. Soc.*, 1961, 83, 2909.
78. Gatlin, L., and Davis, J. C., *J. Am. Chem. Soc.*, 1962, 84, 4464.
79. Kokko, J. P., Mandell, L., and Golgstein, J. H., *J. Am. Chem. Soc.*, 1962, 84, 1042.
80. Jardetzky, O., Pappas, P., and Warde, N. G., *J. Am. Chem. Soc.*, 1965, 87, 5439.
81. Robert, B. W., Lambert, J. B., and Roberts, J. D., *J. Am. Chem. Soc.*, 1965, 87, 5138.
82. Cushley, R. J., Wempem, I., and Fox, J. J., *J. Am. Chem. Soc.*, 1968, 90, 709.
83. Jeffrey, G. A., and Kinoshita, Y., *Acta Crystallogr.*, 1963, 16, 20.

84. Barker, D. L., and Marsh, R. E., *Acta Crystallogr.*, 1964, 17, 1581.
85. McClure, R. J., and Craven, B. M., *Acta Crystallogr.*, 1973, 29B, 1234.
86. Haschemeyer, A. E. V., and Sobell, H. M., *Acta Crystallogr.*, 1965, 19, 125.
87. O'Brien, E. J., *Acta Crystallogr.*, 1967, 23, 92.
88. O'Brien, E. J., *J. Mol. Biol.*, 1966, 22, 377.
89. Voet, D., and Rich, A., *J. Am. Chem. Soc.*, 1969, 91, 3069.
90. Kim, S. H., and Rich, A., *J. Mol. Biol.*, 1969, 42, 87.
91. Sundaralingam, M., and Carrabine, J. A., *J. Mol. Biol.*, 1971, 61, 287.
92. Furberg, S., Peterson, C. S., and Romming, C., *Acta Crystallogr.*, 1965, 18, 313.
93. Coulter, C. L., *J. Am. Chem. Soc.*, 1950, 72, 479.
94. Blout, E. R., and Fields, M., *J. Am. Chem. Soc.*, 1950, 72, 520.
95. Stimson, M. M., and O'Donnell, M. J., *J. Am. Chem. Soc.*, 1952, 14, 1805.
96. Thompson, H. W., Nicholson, D. L., and Shoet, L. N., *Discuss. Faraday Soc.*, 1950, 9, 222.
97. Miles, H. T., *Biochim. Biophys. Acta*, 1959, 35, 274.
98. Miles, H. T., *Proc. Natl. Acad. Sci. U. S. A.*, 1961, 47, 791.
99. Tsuboi, M., Kyoguku, Y., and Shimanouchi, T., *Biochim. Biophys. Acta*, 1962, 55, 1.
100. Miles, H. T., *J. Am. Chem. Soc.*, 1963, 85, 1007.
101. Ulbricht, T. L. V., *Tetrahedron Lett.*, 1963, 16, 1027.

102. Tsuboi, M. and Takahashi, S., in "Physico-Chemical Properties of Nucleic Acids" (Academic Press, New York, London) 1973, 2, 92.
103. Kwiatkowski, J. S., and Pullman, B., Adv. Heterocycl. Chem., 1975, 18, 200.
104. Dreyfus, M., Besnaude, O., Dodin, G., and Dubois, J. E., J. Am. Chem. Soc., 1976, 98, 6339.
105. Watson, D. G., Sweet, R. M., and Marsh, R. E., Acta Crystallogr., 1965, 19, 573.
106. Pullman, B., Berthod, H., Bergmann, F., and Nieman, Z., Tetrahedron, 1970, 26, 1483.
107. Reichman, U., Bergmann, F., Lichtenberg, D., and Nieman, Z., J. Chem. Soc., (Perkin I), 1973, 793.
108. Pugmire, R. J., and Grant, D. M., J. Am. Chem. Soc., 1971, 93, 1880.
109. Hoogsteen, K., Acta Crystallogr., 1963, 16, 950.
110. Stewart, R. F., and Hensen, L. H., J. Chem. Phys., 1964, 40, 2071.
111. Mathews, F. S., and Rich, A., J. Mol. Biol., 1964, 8, 89.
112. Blakagina, Y. G., Volkenshtein, M. D., and Kondrashev, Y. D., Zh. Strukt. Khim., 1966, 7, 399.
113. Katz, L., Tomita, K. I., and Rich, A., Acta Crystallogr., 1966, 21, 754.
114. Tomita, K. I., Katz, L., and Rich, A., J. Mol. Biol., 1967, 30, 545.
115. Kim, S. H., and Rich, A., Proc. Natl. Acad. Sci. U. S. A., 1968, 60, 402.
116. Lai, T. F., and Marsh, R. E., Acta Crystallogr., 1972, 28B, 1982.
117. Watson, D. G., Sutton, D. J., and Tollin, P., Acta Crystallogr., 1965, 19, 111.
118. Rao, S. T., and Sundaralingam, M., J. Am. Chem. Soc., 1970, 92, 4963.

119. Rohrer, D. C., and Sundaralingam, M., J. Am. Chem. Soc., 1970, 92, 4956.
120. Shikata, K., Ueki, T., and Mitsui, T., Acta Crystallogr., 1973, 29B, 31.
121. Chwang, A. K., Sundaralingam, M., and Hanessian, S., Acta Crystallogr., 1974, 30B, 2273.
122. Lord, R. C., and Thomas, G. J., Spectrochim. Acta, 1967, 23A, 2551.
123. Kyoguku, Y., Higuchi, S., and Tsuboi, M., Spectrochim. Acta, 23A, 969.
124. Lautie, E., and Novak, A., J. Chim. Phys., 1974, 71, 415.
125. Pal, B. C., and Horton, C. A., J. Chem. Soc., 1964, Part 1, 400.
126. Montgomery, J. A., and Thomas, G. H., J. Heterocycl. Chem., 1964, 1, 221.
127. Wolfenden, R. V., J. Mol. Biol., 1969, 40, 307.
128. Mason, S. F., in "Chemistry and Biology of Purines" (Ciba Found. Symp., London) 1957, p. 60.
129. Mason, S. F., J. Chem. Soc., 1957, Part 4, 4874.
130. Lister, J. H., Adv. Heterocycl. Chem., 1966, 6, 1.
131. Kleinwachter, V., Drobnick, J., And Augustin, L., Photochem. Photobiol., 1967, 6, 133.
132. Sukhorukov, B. J., and Poltev, V. I., Biophysics, 1964, 9, 152.
133. Berthod, H., Geisner-Prettre, C., and Pullman, A., C. R. Sci, 1966, 262, 2657.
134. Katritzky, A. R., and Lagowski, J., Adv. Heterocycl. Chem, 1963, 2, 58.
135. Weiler-Feilchenfeld, H., and Nieman, Z., J. Chem. Soc., 1970, Part, B, 1334.
136. Pullman, B., Bergmann, E. D., Weiler-Felchenfeld, H., and Nieman, Z., Int. J. Quantum Chem., 1969, 35, 103.
137. Chen, H. H., aand Clark, L. B., J. Chem. Phys., 1969, 51, 1862.

138. Thewalt, U., Bugg, C. E., and Marsh, R. E., *Acta Crystallogr.*, 1971, 27B, 2358.
139. Delabar, J. M., and Majoube, M., *Spectrochim. Acta*, 1978, 34A, 129.
140. Tsuboi, M., and Kyogoku, Y., in "Synthetic Procedures in Nucleic Acid Chemistry" (John Wiley & Sons, Inc., New York) 1973, 2, 215.
141. Meyer, B., in "Low-Temperature Spectroscopy" (American Elsevier Publishing Company, Inc, New York) 1971.
142. Durig, J. R., and Sullivan, J. F., in "Matrix-Isolation Spectroscopy" (D. Reidel Publishing Company, Dordrecht, Boston, London) 1981, p. 403.
143. Barnes, A. J., *J. Mol. Struct.*, 1984, 113, 161.
144. Van Thiel, M., Becker, E. D., and Pimentel, G. C., *J. Chem. Phys.*, 1957, 27, 486.
145. Van Thiel, M., Becker, E. D., and Pimentel, G. C., *J. Chem. Phys.*, 1957, 27, 95.
146. Barnes, A. J., in "Matrix-Isolation Spectroscopy" (D. Reidel Publishing Company, Dordrecht, Boston, London) 1981, p. 13.
147. Barnes, A. J., LeGall, L., Madec, C., and Lauransan, J., *J. Mol. Struct.*, 1977, 38, 109.
148. Walsh, B., Barnes, A. J., Suzuki, S., and Orville-Thomas, W. J., *J. Mol. Spectry.*, 1978, 60, 343.
149. Barnes, A. J., *J. Mol. Struct.*, 1980, 60, 343.
150. Warren, J. A., Smith, G. R., and Guillory, W. A., *J. Chem. Phys.*, 1980, 4091.
151. Carr, B. R., Chadwick, B. M., Edward, C. S., Long, P. A., and Wharton, G. C., *J. Mol. Struct.*, 1980, 62, 291.
152. Latajka, Z., Person, W. B., and Morokuma, K., *J. Mol., Struct. (Theochem.)*, 1986, 135, 253.
153. Nishimura, Y., Tsuboi, M., Kato, S., and Morokuma, K., *Bull. Chem. Soc. Jpn.*, 1985, 58, 638.

154. Szczesniak, M., Ph.D. Thesis, Polish Academy of Sciences (Warsaw, Poland) 1985.
155. Coleman, W. M., and Gordon, B. M., Appl. Spectrosc., 1987, 41, 1159.
156. Coleman, W. M., and Gordon, B. M., Appl. Spectrosc., 1987, 41, 1163.
157. Watson, J. D., in "Molecular Biology of the Gene" (W. A. Benjamin, Inc., New York) 1976.

BIOGRAPHICAL SKETCH

Luis A. Hernandez-Villarini was born in Ponce, Puerto Rico. He received a B. S. degree in chemistry from the University of Puerto Rico at Mayaguez. After serving his tour of duty with the armed forces, he returned to Puerto Rico and obtained a M. S. degree from his alma mater. After graduation in May 1980, he remained at the University of Puerto Rico as an instructor of physical chemistry laboratories. Admitted to the Graduate School at the University of Florida in August 1981, he received his Ph.D. degree in physical chemistry in December 1987.

Mr. Hernandez-Villarini is married to the former Mayra L. Soto.

I certify that I have read this study and that in my opinion it conforms to acceptable standards of scholarly presentation and is fully adequate, in scope and quality, as a dissertation for the degree of Doctor of Philosophy.

Willis B. Person
Willis B. Person, Chairman
Professor of Chemistry

I certify that I have read this study and that in my opinion it conforms to acceptable standards of scholarly presentation and is fully adequate, in scope and quality, as a dissertation for the degree of Doctor of Philosophy.

Martin Vala
Martin Vala
Professor of Chemistry

I certify that I have read this study and that in my opinion it conforms to acceptable standards of scholarly presentation and is fully adequate, in scope and quality, as a dissertation for the degree of Doctor of Philosophy.

Robert J. Hanrahan
Robert J. Hanrahan
Professor of Chemistry

I certify that I have read this study and that in my opinion it conforms to acceptable standards of scholarly presentation and is fully adequate, in scope and quality, as a dissertation for the degree of Doctor of Philosophy.

A. Bratton-Toth
Anna Bratton-Toth
Assistant Professor of Chemistry

I certify that I have read this study and that in my opinion it conforms to acceptable standards of scholarly presentation and is fully adequate, in scope and quality, as a dissertation for the degree of Doctor of Philosophy.

Stephen Schulman
Stephen Schulman
Professor of Pharmacy

This dissertation was submitted to the Graduate Faculty of the Department of Chemistry in the College of Liberal Arts and Sciences and to the Graduate School and was accepted as partial fulfillment of the requirements for the degree of Doctor of Philosophy.

December 1987

Dean, Graduate School